View metadata, citation and similar papers at core.ac.uk

brought to you by CORE

provided by Elektronische Publikationen der Universität Hohenheim

UNIVERSITY OF HOHENHEIM

FACULTY OF BUSINESS, ECONOMICS AND SOCIAL SCIENCES

HOHENHEIM DISCUSSION PAPERS

IN BUSINESS, ECONOMICS AND SOCIAL SCIENCES

Institute of Economics

DISCUSSION PAPER 13-2015

A DATA–CLEANING AUGMENTED KALMAN FILTER FOR ROBUST ESTIMATION OF STATE SPACE MODELS

Martyna Marczak,

University of Hohenheim

Tommaso Proietti,

Università di Roma “Tor Vergata”, Italy

CREATES, Denmark

Stefano Grassi,

University of Kent,

United Kingdom

State: October 2015

www.wiso.uni-hohenheim.de

Discussion Paper 13-2015

A Data–Cleaning Augmented Kalman Filter for Robust Estimation of State Space Models

Martyna Marczak
Tommaso Proietti
Stefano Grassi

Download this Discussion Paper from our homepage:

https://wiso.uni-hohenheim.de/papers

ISSN 2364-2076 (Printausgabe)
ISSN 2364-2084 (Internetausgabe)

Die Hohenheim Discussion Papers in Business, Economics and Social Sciences dienen der schnellen Verbreitung von Forschungsarbeiten der Fakultät Wirtschafts- und Sozialwissenschaften. Die Beiträge liegen in alleiniger Verantwortung der Autoren und stellen nicht notwendigerweise die Meinung der Fakultät Wirtschafts- und Sozialwissenschaften dar.

Hohenheim Discussion Papers in Business, Economics and Social Sciences are intended to make results of the Faculty of Business, Economics and Social Sciences research available to the public in order to encourage scientific discussion and suggestions for revisions. The authors are solely responsible for the contents which do not necessarily represent the opinion of the Faculty of Business, Economics and Social Sciences.

A Data–Cleaning Augmented Kalman Filter for Robust Estimation of State Space Models

Martyna Marczak*
University of Hohenheim, Germany

Tommaso Proietti†
Università di Roma "Tor Vergata", Italy, and CREATES, Denmark

Stefano Grassi‡
University of Kent, United Kingdom

Abstract

This article presents a robust augmented Kalman filter that extends the data– cleaning filter (Masreliez and Martin, 1977) to the general state space model featuring nonstationary and regression effects. The robust filter shrinks the observations towards their one–step–ahead prediction based on the past, by bounding the effect of the information carried by a new observation according to an influence function. When maximum likelihood estimation is carried out on the replacement data, an M–type estimator is obtained. We investigate the performance of the robust AKF in two applications using as a modeling framework the basic structural time series model, a popular unobserved components model in the analysis of seasonal time series. First, a Monte Carlo experiment is conducted in order to evaluate the comparative accuracy of the proposed method for estimating the variance parameters. Second, the method is applied in a forecasting context to a large set of European trade statistics series.

JEL Classification: C32, C53, C63

Keywords: robust filtering, augmented Kalman filter, structural time series model, additive outlier, innovation outlier

*Corresponding author: University of Hohenheim, Department of Economics, Schloss, Museumsfluegel, D-70593 Stuttgart, Germany. E-mail: marczak@uni-hohenheim.de.

†Dipartimento di Economia e Finanza, Università di Roma Tor Vergata, Via Columbia 2, 00133 Rome, Italy. E-mail: tommaso.proietti@uniroma2.it.
Tommaso Proietti acknowledges support from CREATES - Center for Research in Econometric Analysis of Time Series (DNRF78), funded by the Danish National Research Foundation.
‡School of Economics, University of Kent, United Kingdom. E-mail: S.Grassi@kent.ac.uk.

1 Introduction

State space models and the Kalman filter offer a powerful tool for statistical analysis of time series. Any linear Markovian time series model can be put into a state space form and then the Kalman filter can be applied to estimate the model parameters by maximum likelihood via the prediction error decomposition. However, if the considered series is contaminated by outliers, the estimated parameters might be strongly biased. Masreliez and Martin (1977) proposed a robustification of the Kalman filter to remove the outlier effects. This approach relies on scaling residuals by an influence function, a continuous and bounded function, so that the estimator resulting from the application of the robust Kalman filter belongs to the class of M–estimators. Martin (1979) and Martin and Thomson (1982) are early works examining the robust Kalman filter in the case of ARMA models. A comprehensive account is provided in chapter 8 of Maronna et al. (2006). Recent extensions of the original robust Kalman filter include algorithms developed by, e.g., Liu et al. (2004), Gandhi and Mili (2010) and Ruckdeschel et al. (2014). So far, the robust Kalman filter has been derived in a stationary setting.

In this paper we propose another extension of the robust Kalman filter which is suited for nonstationary series and/or models capturing regressor effects. In particular, we build on the augmented Kalman filter (AKF) proposed by de Jong (1991). To the best of our knowledge, this is the first paper that combines the AKF with a robustification procedure.

Our approach is based on the heuristic argument of shrinking a suspect observation towards its one-step-ahead prediction so as to achieve robustness. A theoretically consistent and empirically viable approach to robustness in time series analysis has been recently proposed by Harvey (2013). The approach, however, deals with unobserved components whose dynamics is driven by the conditional score of the observation density and, unlike our proposed method, cannot handle models with multiple source of errors.

Since the presented approach – the robust AKF – might be of relevance for economic time series many of which are nonstationary and affected by outlying observations, we consider the class of structural time series models, i.e. models formulated in terms of unobserved components, like trend, cycle, seasonal or irregular components, inherent in many economic time series (Harvey, 1989). To account for the fact that treatment of outliers usually accompanies the removal of the seasonal component from the data, as the reference model we use the basic structural model (BSM) for univariate series (Harvey and Todd, 1983), often applied for the purpose of seasonal adjustment. The BSM is a simple yet flexible model providing a satisfactory fit to a wide range of seasonal time series.

Using the BSM as the modeling framework, we investigate the performance of the

robust AKF in a Monte Carlo simulation exercise and in an empirical application. In the Monte Carlo experiment, the simulated series are affected by additive or innovation outliers. Our results complement and extend Bianco et al. (2001), in that we assess the role of specific outlier types on estimating the correct size of a particular variance component in a nonstationary dynamic regression framework. In the empirical application, we conduct a pseudo real–time forecasting experiment on a large dataset of 540 monthly European trade statistics series, that are contaminated with additive outliers. The aim of the study is to investigate whether the robust AKF is capable of cleaning the data effectively and thus reducing the forecast uncertainty.

The remainder of the article is organized as follows. In Section 2, we set out the reference state space form and we present the AKF. The robust AKF is exposed in Section 3. Section 4 presents the modeling framework used in the application part of the study. In Section 5, we evaluate the robust AKF by means of a Monte Carlo experiment whereas in Section 6 we discuss the results of the forecasting exercise. Section 7 concludes.

2 The Augmented Kalman Filter

The augmented Kalman filter, see Rosenberg (1973) and de Jong (1991), is an essential tool for likelihood inferences on the parameters of a state space model and for linear prediction. Given the parameter values, it evaluates the likelihood via the prediction error decomposition, and once the parameters are estimated as the maximizers of the likelihood function, it enables the out–of–sample prediction of the series and the estimation of the states in real time.

2.1 State space form

Consider a multivariate time series $\mathbf{y}_t$ with N elements. The state space model for $\mathbf{y}_t$ is given by:

$$\begin{aligned} \mathbf{y}_t &= \mathbf{Z}_t\boldsymbol{\alpha}_t + \mathbf{X}_t\boldsymbol{\beta} + \mathbf{G}_t\boldsymbol{\varepsilon}_t,\ \boldsymbol{\varepsilon}_t \sim \mathrm{N}(\mathbf{0}, \sigma^2\mathbf{I}), \\ \boldsymbol{\alpha}_{t+1} &= \mathbf{T}_t\boldsymbol{\alpha}_t + \mathbf{W}_t\boldsymbol{\beta} + \mathbf{H}_t\boldsymbol{\varepsilon}_t,\ \ t = 1, ..., n \end{aligned} \tag{1}$$

where $\boldsymbol{\alpha}_t$ is the $(m \times 1)$ state vector, $\mathbf{X}_t$ and $\mathbf{W}_t$ denote fixed and known matrices of dimension $(N \times k)$ and $(m \times k)$, respectively. Vector $\boldsymbol{\beta}$ contains regressor effects and/or initial values of nonstationary elements of $\mathbf{y}_t$. The initial state vector is specified as follows:

$$\boldsymbol{\alpha}_1 = \tilde{\boldsymbol{\alpha}}^*_{1|0} + \mathbf{W}_0\boldsymbol{\beta} + \mathbf{H}_0\boldsymbol{\varepsilon}_0, \tag{2}$$

where $\tilde{\boldsymbol{\alpha}}^*_{1|0}$, $\mathbf{W}_0$, and $\mathbf{H}_0$ are known quantities.

The leading case of interest is when $\boldsymbol{\beta}$ is partitioned as

$$\boldsymbol{\beta} = \begin{bmatrix} \boldsymbol{\alpha}_0^\dagger \\ \boldsymbol{\beta}_x \\ \boldsymbol{\beta}_w \end{bmatrix}, \quad \begin{aligned} \mathbf{X}_t &= \left[\mathbf{0}, \mathbf{X}_t^\dagger, \mathbf{0}\right], \\ \mathbf{W}_t &= \left[\mathbf{0}, \mathbf{0}, \mathbf{W}_t^\dagger\right], \\ \mathbf{W}_0 &= \left[\mathbf{T}^\dagger, \mathbf{0}, \mathbf{W}_0^\dagger\right], \end{aligned}$$

where $\boldsymbol{\alpha}_0^\dagger$ is a subset of initial states corresponding to nonstationary elements of $\boldsymbol{\alpha}_t$, $\mathbf{X}_t^\dagger$ is an $(N \times k_x)$ matrix of explanatory variables affecting the response variable, $\mathbf{W}_t^\dagger$ is an $(m \times k_w)$ matrix of explanatory variables affecting $\boldsymbol{\alpha}_{t+1}$, and $\mathbf{T}^\dagger$ is a matrix relating $\boldsymbol{\alpha}_1$ to $\boldsymbol{\alpha}_0^\dagger$.

The vector $\boldsymbol{\beta}$ can be considered as fixed (and unknown), or as a random vector with a diffuse distribution, $\boldsymbol{\beta} \sim \mathrm{N}(\mathbf{0}, \boldsymbol{\Sigma}_\beta)$, where $\boldsymbol{\Sigma}_\beta^{-1} \to \mathbf{0}$.

2.2 Recursions

Consider the state space model (1), with initial conditions stated in (2). Setting $\mathbf{A}_{1|0} = -\mathbf{W}_0$ and $\mathbf{P}^*_{1|0} = \mathbf{H}_0\mathbf{H}_0'$, the AKF is, for $t = 1, \ldots, n$:

$$\begin{aligned} &\boldsymbol{\nu}_t^* = \mathbf{y}_t - \mathbf{Z}_t\tilde{\boldsymbol{\alpha}}^*_{t|t-1}, && \mathbf{V}_t = \mathbf{X}_t - \mathbf{Z}_t\mathbf{A}_{t|t-1}, \\ &\mathbf{F}_t^* = \mathbf{Z}_t\mathbf{P}^*_{t|t-1}\mathbf{Z}_t' + \mathbf{G}_t\mathbf{G}_t', && \mathbf{K}_t^* = (\mathbf{T}_t\mathbf{P}^*_{t|t-1}\mathbf{Z}_t' + \mathbf{H}_t\mathbf{G}_t')\mathbf{F}_t^{*-1}, \\ &\tilde{\boldsymbol{\alpha}}^*_{t+1|t} = \mathbf{T}_t\tilde{\boldsymbol{\alpha}}^*_{t|t-1} + \mathbf{K}_t^*\boldsymbol{\nu}_t^*, && \mathbf{A}_{t+1|t} = \mathbf{T}_t\mathbf{A}_{t|t-1} - \mathbf{W}_t + \mathbf{K}_t^*\mathbf{V}_t, \\ &\mathbf{P}^*_{t+1|t} = \mathbf{T}_t\mathbf{P}^*_{t|t-1}\mathbf{T}_t' + \mathbf{H}_t\mathbf{H}_t' - \mathbf{K}_t^*\mathbf{F}_t^*\mathbf{K}_t^{*\prime}. \end{aligned} \tag{3}$$

The starred quantities correspond to the usual Kalman filter applied to $\mathbf{y}_t$ with $\boldsymbol{\beta} = \mathbf{0}$, when the nonstationary initial effects are set to zero and no explanatory variables are considered (i.e. using the initial condition $\tilde{\boldsymbol{\alpha}}^*_{1|0}$). The individual columns of the matrices $\mathbf{V}_t$ and $\mathbf{A}_{t+1|t}, t = 1, \ldots, n$, arise from running to each of the columns of $\mathbf{X}_t$ and $\mathbf{A}_{t|t-1}$, respectively, analogous recursions as for $\mathbf{y}_t$ and $\tilde{\boldsymbol{\alpha}}^*_{t+1|t}$.

Defining

$$\mathbf{s}_t = \sum_{i=1}^{t} \mathbf{V}_i'\mathbf{F}_i^{*-1}\boldsymbol{\nu}_i^*, \qquad \mathbf{S}_t = \sum_{i=1}^{t} \mathbf{V}_i'\mathbf{F}_i^{*-1}\mathbf{V}_i,$$

for $t \geq k$ we obtain

$$\tilde{\boldsymbol{\beta}}_{t|t-1} = \mathbf{S}_{t-1}^{-1}\mathbf{s}_{t-1}$$

as the estimate of $\boldsymbol{\beta}$ using the information set up to the period $t-1$, $\{\boldsymbol{\mathcal{Y}}_{t-1}, \boldsymbol{\mathcal{X}}_{t-1}, \boldsymbol{\mathcal{W}}_{t-1}\}$, where $\boldsymbol{\mathcal{Y}}_{t-1}$, $\boldsymbol{\mathcal{X}}_{t-1}$, and $\boldsymbol{\mathcal{W}}_{t-1}$ include $\mathbf{y}_i$, $\mathbf{X}_i$ and $\mathbf{W}_i$, respectively, up to $i = t-1$.

If $\boldsymbol{\beta}$ is considered as a fixed vector, then $\tilde{\boldsymbol{\beta}}_{t|t-1}$ is its generalized least square (GLS) estimator using the observations up to time $t-1$. The covariance matrix of the regression coefficients is $\mathbf{B}_{t|t-1} = \sigma^2\mathbf{S}_{t-1}^{-1}$. In the diffuse case, $\tilde{\boldsymbol{\beta}}_{t|t-1}$ represents the mean of the posterior distribution, see de Jong (1991), and $\sigma^2\mathbf{S}_{t-1}^{-1}$ represents its posterior covariance matrix.

The innovations, $\boldsymbol{\nu}_t = \mathbf{y}_t - \mathrm{E}(\mathbf{y}_t|\boldsymbol{\mathcal{Y}}_{t-1}, \boldsymbol{\mathcal{X}}_{t-1}, \boldsymbol{\mathcal{W}}_{t-1})$, the one–step–ahead prediction of the state vector, $\tilde{\boldsymbol{\alpha}}_{t|t-1} = \mathrm{E}(\boldsymbol{\alpha}_t|\boldsymbol{\mathcal{Y}}_{t-1}, \boldsymbol{\mathcal{X}}_{t-1}, \boldsymbol{\mathcal{W}}_{t-1})$, and the corresponding estimation error covariance matrices are

$$\begin{array}{rclcrcl} \boldsymbol{\nu}_t & = & \boldsymbol{\nu}_t^* - \mathbf{V}_t\tilde{\boldsymbol{\beta}}_{t|t-1}, & & \mathbf{F}_t & = & \mathbf{F}_t^* + \mathbf{V}_t\mathbf{B}_{t|t-1}\mathbf{V}_t', \\ \tilde{\boldsymbol{\alpha}}_{t|t-1} & = & \tilde{\boldsymbol{\alpha}}_{t|t-1}^* - \mathbf{A}_{t|t-1}\tilde{\boldsymbol{\beta}}_{t|t-1}, & & \mathbf{P}_{t|t-1} & = & \mathbf{P}_{t|t-1}^* + \mathbf{A}_{t|t-1}\mathbf{B}_{t|t-1}\mathbf{A}_{t|t-1}'. \end{array} \tag{4}$$

2.3 Real–time estimates and predictions

As $\mathbf{S}_t = \mathbf{S}_{t-1} + \mathbf{V}_t'\mathbf{F}_t^*\mathbf{V}_t$, by the Sherman–Woodbury–Morrison matrix inversion lemma (Henderson and Searle, 1981),

$$\mathbf{S}_t^{-1} = \mathbf{S}_{t-1}^{-1} - \mathbf{S}_{t-1}^{-1}\mathbf{V}_t'\left(\mathbf{F}_t^* + \mathbf{V}_t\mathbf{S}_{t-1}^{-1}\mathbf{V}_t'\right)^{-1}\mathbf{V}_t\mathbf{S}_{t-1}^{-1}.$$

The updated or, in other words, real–time estimate of the vector $\boldsymbol{\beta}$ is $\tilde{\boldsymbol{\beta}}_{t|t} = \mathbf{S}_t^{-1}\mathbf{s}_t$. In view of $\mathbf{s}_t = \mathbf{s}_{t-1} + \mathbf{V}_t'\mathbf{F}_t^*\boldsymbol{\nu}_t^*$, the above matrix inverse, and recalling (4), $\tilde{\boldsymbol{\beta}}_{t|t}$ can be written, after some algebra, as:

$$\tilde{\boldsymbol{\beta}}_{t|t} = \tilde{\boldsymbol{\beta}}_{t|t-1} + \mathbf{B}_{t|t-1}\mathbf{V}_t'\mathbf{F}_t^{-1}\boldsymbol{\nu}_t.$$

The updated covariance matrix is

$$\mathbf{B}_{t|t} = \mathbf{B}_{t|t-1} - \mathbf{B}_{t|t-1}\mathbf{V}_t'\mathbf{F}_t^{-1}\mathbf{V}_t\mathbf{B}_{t|t-1}.$$

The updated estimates of the state vector, $\tilde{\boldsymbol{\alpha}}_{t|t} = \mathrm{E}(\boldsymbol{\alpha}_t|\boldsymbol{\mathcal{Y}}_t, \boldsymbol{\mathcal{X}}_t, \boldsymbol{\mathcal{W}}_t)$, and their covariance matrix $\mathrm{Var}(\boldsymbol{\alpha}_t|\boldsymbol{\mathcal{Y}}_t, \boldsymbol{\mathcal{X}}_t, \boldsymbol{\mathcal{W}}_t) = \sigma^2\mathbf{P}_{t|t}$ are:

$$\begin{array}{rcl} \tilde{\boldsymbol{\alpha}}_{t|t} & = & \tilde{\boldsymbol{\alpha}}_{t|t-1}^* - \mathbf{A}_{t|t-1}\tilde{\boldsymbol{\beta}}_{t|t} + \mathbf{P}_{t|t-1}^*\mathbf{Z}_t'\mathbf{F}_t^{*-1}(\boldsymbol{\nu}_t^* - \mathbf{V}_t\tilde{\boldsymbol{\beta}}_{t|t}), \\ \mathbf{P}_{t|t} & = & \mathbf{P}_{t|t-1}^* - \mathbf{P}_{t|t-1}^*\mathbf{Z}_t'\mathbf{F}_t^{*-1}\mathbf{Z}_t\mathbf{P}_{t|t-1}^* + \mathbf{A}_{t|t}\mathbf{B}_{t|t}\mathbf{A}_{t|t}'. \end{array} \tag{5}$$

The GLS residual can be rewritten in terms of the innovations:

$$\boldsymbol{\nu}_t^* - \mathbf{V}_t\tilde{\boldsymbol{\beta}}_{t|t} = \mathbf{F}_t^*\mathbf{F}_t^{-1}\boldsymbol{\nu}_t,$$

so that

$$\tilde{\boldsymbol{\alpha}}_{t|t} = \tilde{\boldsymbol{\alpha}}_{t|t-1}^* - \mathbf{A}_{t|t-1}\tilde{\boldsymbol{\beta}}_{t|t} + \mathbf{P}_{t|t-1}^*\mathbf{Z}_t'\mathbf{F}_t^{-1}\boldsymbol{\nu}_t. \tag{6}$$

Finally, denoting $\tilde{\boldsymbol{\varepsilon}}_{t|t} = \mathrm{E}(\boldsymbol{\varepsilon}_t|\boldsymbol{\mathcal{Y}}_t, \boldsymbol{\mathcal{X}}_t, \boldsymbol{\mathcal{W}}_t)$,

$$\begin{aligned} \tilde{\boldsymbol{\varepsilon}}_{t|t} &= \mathbf{G}_t'\mathbf{F}_t^{*-1}(\boldsymbol{\nu}_t^* - \mathbf{V}_t\tilde{\boldsymbol{\beta}}_{t|t}) \\ &= \mathbf{G}_t'\mathbf{F}_t^{-1}\boldsymbol{\nu}_t. \end{aligned} \tag{7}$$

Notice that the same real–time estimates would be obtained from

$$\begin{aligned} &\tilde{\boldsymbol{\alpha}}_{t|t}^* = \tilde{\boldsymbol{\alpha}}_{t|t-1}^* + \mathbf{P}_{t|t-1}^*\mathbf{Z}_t'\mathbf{F}_t^{*-1}\boldsymbol{\nu}_t^*, \qquad \mathbf{A}_{t|t} = \mathbf{A}_{t|t-1} + \mathbf{P}_{t|t-1}^*\mathbf{Z}_t'\mathbf{F}_t^{*-1}\mathbf{V}_t, \\ &\mathbf{P}_{t|t}^* = \mathbf{P}_{t|t-1}^* - \mathbf{P}_{t|t-1}^*\mathbf{Z}_t'\mathbf{F}_t^{*-1}\mathbf{Z}_t\mathbf{P}_{t|t-1}^* \end{aligned} \tag{8}$$

setting

$$\tilde{\boldsymbol{\alpha}}_{t|t} = \tilde{\boldsymbol{\alpha}}_{t|t}^* - \mathbf{A}_{t|t}\tilde{\boldsymbol{\beta}}_{t|t}, \quad \mathbf{P}_{t|t} = \mathbf{P}_{t|t}^* + \mathbf{A}_{t|t}\mathbf{B}_{t|t}\mathbf{A}_{t|t}'. \tag{9}$$

For the regression coefficients set $\tilde{\boldsymbol{\beta}}_{t+1|t} = \tilde{\boldsymbol{\beta}}_{t|t}$ and $\mathbf{B}_{t+1|t} = \mathbf{B}_{t|t}$. When $\mathbf{H}_t\mathbf{G}_t' = \mathbf{0}$, the prediction step for the state vector gives:

$$\begin{aligned} &\tilde{\boldsymbol{\alpha}}_{t+1|t}^* = \mathbf{T}_t\tilde{\boldsymbol{\alpha}}_{t|t}^*, \qquad \mathbf{A}_{t+1|t} = \mathbf{T}_t\mathbf{A}_{t|t} - \mathbf{W}_t, \\ &\mathbf{P}_{t+1|t}^* = \mathbf{T}_t\mathbf{P}_{t|t}^*\mathbf{T}_t' + \mathbf{H}_t\mathbf{H}_t' \end{aligned} \tag{10}$$

3 The Robust Augmented Kalman Filter

To control for the effects of outliers, the AKF equations in Section 2 are modified using an influence function applied to the standardized innovations.

Let $\mathbf{u}_t = \mathbf{F}_t^{-1/2}\boldsymbol{\nu}_t$ denote the standardized innovations; further, let $\psi(u_{it})$ denote the influence function of a standardized innovation $u_{it}, i = 1, \ldots, N$, and $w(u_{it}) = \psi(u_{it})/u_{it}$ be the corresponding weight function. Moreover, let $\boldsymbol{\psi}(\mathbf{u}_t) = (\psi(u_{1i}), \ldots, \psi(u_{Nt}))'$ and $\mathbf{w}(\mathbf{u}_t) = \mathrm{diag}\,(w(u_{1i}), \ldots, w(u_{Nt}))$.

An influence function is a piecewise continuous bounded function $\psi : \mathbb{R} \to \mathbb{R}$, such that $\psi(-u) = -\psi(u)$, $\psi(u) = u$ for $|u| \leq c$, and $|\psi(u)|$ is bounded for $|u| > c$. For redescending functions, $\lim_{|u|\to\infty}\psi(u) = d = 0$, so that the effect of high values of u is zero, whereas for monotone non–decreasing functions the effect is bounded by a constant d, i.e. $|\psi(u)| \leq d$, for $u > d > 0$. Details on the specific form of the influence function considered in this paper are postponed to Section 3.2.

Assume also that at the $t = k$–th update, all the AKF quantities have been computed and the following inferences are available: $\tilde{\boldsymbol{\beta}}_{k|k} = \tilde{\boldsymbol{\beta}}_{k+1|k} = \mathbf{S}_k^{-1}\mathbf{s}_k$. Then, for $t = k +$

$1, \ldots, n$, the robust AKF is given by:

$$\begin{array}{ll} \boldsymbol{\nu}_t^* = \mathbf{y}_t - \mathbf{Z}_t\tilde{\boldsymbol{\alpha}}_{t|t-1}^*, & \mathbf{V}_t = \mathbf{X}_t - \mathbf{Z}_t\mathbf{A}_{t|t-1}, \\ \mathbf{F}_t^* = \mathbf{Z}_t\mathbf{P}_{t|t-1}^*\mathbf{Z}_t' + \mathbf{G}_t\mathbf{G}_t', & \mathbf{K}_t^* = (\mathbf{T}_t\mathbf{P}_{t|t-1}^*\mathbf{Z}_t' + \mathbf{H}_t\mathbf{G}_t')\mathbf{F}_t^{*-1}, \\ \boldsymbol{\nu}_t = \boldsymbol{\nu}_t^* - \mathbf{V}_t\tilde{\boldsymbol{\beta}}_{t|t-1}, & \mathbf{F}_t = \mathbf{F}_t^* + \mathbf{V}_t\mathbf{B}_{t|t-1}\mathbf{V}_t', \end{array} \tag{11}$$

$$\begin{array}{l} \tilde{\boldsymbol{\beta}}_{t|t} = \tilde{\boldsymbol{\beta}}_{t|t-1} + \mathbf{B}_{t|t-1}\mathbf{V}_t'\mathbf{F}_t^{-1/2}\boldsymbol{\psi}\left(\mathbf{u}_t\right), \\ \mathbf{B}_{t|t} = \mathbf{B}_{t|t-1} - \mathbf{w}(\mathbf{u}_t)\mathbf{B}_{t|t-1}\mathbf{V}_t'\mathbf{F}_t^{-1}\mathbf{V}_t\mathbf{B}_{t|t-1}, \end{array} \tag{12}$$

$$\begin{array}{l} \tilde{\boldsymbol{\alpha}}_{t|t} = \tilde{\boldsymbol{\alpha}}_{t|t-1}^* - \mathbf{A}_{t|t-1}\tilde{\boldsymbol{\beta}}_{t|t} + \mathbf{P}_{t|t-1}^*\mathbf{Z}_t'\mathbf{F}_t^{-1/2}\boldsymbol{\psi}\left(\mathbf{u}_t\right), \\ \mathbf{P}_{t|t} = \mathbf{P}_{t|t-1}^* - \mathbf{w}(\mathbf{u}_t)\mathbf{P}_{t|t-1}^*\mathbf{Z}_t'\mathbf{F}_t^{*-1}\mathbf{Z}_t\mathbf{P}_{t|t-1}^* + \mathbf{A}_{t|t}\mathbf{B}_{t|t}\mathbf{A}_{t|t}', \end{array} \tag{13}$$

$$\begin{array}{l} \tilde{\boldsymbol{\alpha}}_{t+1|t}^* = \mathbf{T}_t\tilde{\boldsymbol{\alpha}}_{t|t-1}^* + \mathbf{w}(\mathbf{u}_t)\mathbf{K}_t^*\boldsymbol{\nu}_t^*, \\ \mathbf{A}_{t+1|t} = \mathbf{T}_t\mathbf{A}_{t|t-1} - \mathbf{W}_t + \mathbf{w}(\mathbf{u}_t)\mathbf{K}_t^*\mathbf{V}_t, \\ \mathbf{P}_{t+1|t}^* = \mathbf{T}_t\mathbf{P}_{t|t-1}^*\mathbf{T}_t' + \mathbf{H}_t\mathbf{H}_t' - \mathbf{w}(\mathbf{u}_t)\mathbf{K}_t^*\mathbf{F}_t^*\mathbf{K}_t^{*'}. \end{array} \tag{14}$$

Equations (11) are the usual AKF equations for computing the innovations and their covariance matrix (up to a scale factor). Equations (12) shrink the real–time estimate of the coefficient vector $\boldsymbol{\beta}$ towards $\tilde{\boldsymbol{\beta}}_{t|t-1} + \mathbf{C}_t\mathbf{d}$, where $\mathbf{C}_t = \mathbf{B}_{t|t-1}\mathbf{V}_t'\mathbf{F}_t^{-1/2}$; for $\mathbf{d} = \mathbf{0}$ this corresponds to the one–step–ahead prediction $\tilde{\boldsymbol{\beta}}_{t|t-1}$. The covariance matrix is adjusted accordingly, i.e. the estimation error variance is reduced by a smaller amount depending on the size of the standardized innovations. Equations (13) provide the robust real–time estimate of the state vector at time t: if $\boldsymbol{\psi}(\mathbf{u}_t) \to \mathbf{d}$, $\tilde{\boldsymbol{\alpha}}_{t|t} \to \tilde{\boldsymbol{\alpha}}_{t|t-1} + \mathbf{D}_t\mathbf{d}$, where $\mathbf{D}_t = \mathbf{P}_{t|t-1}^*\mathbf{Z}_t'\mathbf{F}_t^{-1/2} - \mathbf{A}_{t|t-1}\mathbf{C}_t$. If $\mathbf{d} = \mathbf{0}$, then no updating takes place, and no reduction in the state estimation error variance matrix occurs. Finally, the first two equations of (14) are such that if $\mathbf{w}(\mathbf{u}_t) = \mathbf{I}$, $\tilde{\boldsymbol{\alpha}}_{t+1|t}^* - \mathbf{A}_{t+1|t}\tilde{\boldsymbol{\beta}}_{t|t}$ equals the one–step–ahead prediction $\tilde{\boldsymbol{\alpha}}_{t+1|t}$; otherwise, if $\mathbf{w}(\mathbf{u}_t) \to \mathbf{0}$, $\tilde{\boldsymbol{\alpha}}_{t+1|t}^* - \mathbf{A}_{t+1|t}\tilde{\boldsymbol{\beta}}_{t|t} \to \tilde{\boldsymbol{\alpha}}_{t+1|t-1} + (\mathbf{T}_t\mathbf{D}_t - \mathbf{W}_t\mathbf{C}_t)\mathbf{d}$. For $\mathbf{d} = \mathbf{0}$, $\tilde{\boldsymbol{\alpha}}_{t+1|t}^* - \mathbf{A}_{t+1|t}\tilde{\boldsymbol{\beta}}_{t|t}$ tends to the two–step–ahead prediction of the states.

The robust AKF shrinks an outlying observation towards the one–step–ahead prediction $\tilde{\mathbf{y}}_{t|t-1} = \mathbf{Z}_t\tilde{\boldsymbol{\alpha}}_{t|t-1} + \mathbf{X}_t\tilde{\boldsymbol{\beta}}_{t|t-1}$. In particular, it replaces $\mathbf{y}_t = \tilde{\mathbf{y}}_{t|t-1} + \boldsymbol{\nu}_t$ with

$$\mathbf{y}_t^\dagger = \tilde{\mathbf{y}}_{t|t-1} + \mathbf{F}_t^{1/2}\boldsymbol{\psi}(\mathbf{u}_t)$$

Alternatively, this can be written as

$$\mathbf{y}_t^\dagger = \mathbf{Z}_t\tilde{\boldsymbol{\alpha}}_{t|t} + \mathbf{X}_t\tilde{\boldsymbol{\beta}}_{t|t} + \mathbf{G}_t\mathbf{G}_t'\mathbf{F}_t^{-1/2}\boldsymbol{\psi}(\mathbf{u}_t),$$

where $\tilde{\boldsymbol{\alpha}}_{t|t}$ and $\tilde{\boldsymbol{\beta}}_{t|t}$ are as in (13) and (12), respectively, and the last term is the robust counterpart of $\tilde{\boldsymbol{\varepsilon}}_{t|t}$ in eq. (7). In both these versions, $\mathbf{y}_t^\dagger$ is equal to $\mathbf{y}_t$ if $\boldsymbol{\psi}(\mathbf{u}_t) = \mathbf{u}_t$; if,

however, $\boldsymbol{\psi}(\mathbf{u}_t) \to \mathbf{d}$, $\mathbf{y}_t^\dagger$ tends to $\tilde{\mathbf{y}}_{t|t-1} + \mathbf{F}_t^{1/2}\mathbf{d}$, which reduces to the one–step–ahead prediction in the case of $\mathbf{d} = \mathbf{0}$. The sequence $\{\mathbf{y}_t^\dagger\}$, $t = 1, \ldots, n$, represents a cleaned data set which can be used for robust parameter estimation.

3.1 Estimation of model parameters

Estimation of the model parameters $(\boldsymbol{\theta}, \boldsymbol{\beta}, \sigma^2)$ is carried out by maximum likelihood. In particular, we will maximize the diffuse likelihood, defined as

$$L(\boldsymbol{\theta}, \sigma^2) = -\frac{1}{2}\left\{N(n-k)\ln\sigma^2 + \sum \ln|\mathbf{F}_t^*| + \ln|\mathbf{S}_n| + \sigma^{-2}\left[\sum \boldsymbol{\nu}_t^{*\prime}\mathbf{F}_t^{*-1}\boldsymbol{\nu}_t^* - \mathbf{s}_n'\mathbf{S}_n^{-1}\mathbf{s}_n\right], \right\}.$$

The maximum–likelihood (ML) estimator of σ^2 is

$$\hat{\sigma}^2 = \frac{1}{N(n-k)}\left[\sum_{t=1}^{n} \boldsymbol{\nu}_t^{*\prime}\mathbf{F}_t^{*-1}\boldsymbol{\nu}_t^* - \mathbf{s}_n'\mathbf{S}_n^{-1}\mathbf{s}_n\right], \tag{15}$$

and the profile likelihood is

$$L_\sigma(\boldsymbol{\theta}) = -\frac{1}{2}\left[N(n-k)(\ln\hat{\sigma}^2 + 1) + \sum_{t=1}^{n} \ln|\mathbf{F}_t^*| + \ln|\mathbf{S}_n|\right]. \tag{16}$$

The notion of a diffuse likelihood is close to that of a marginal likelihood, being based on reduced rank linear transformation of the series that eliminates dependence on $\boldsymbol{\beta}$; see Francke et al. (2010).

The ML estimator of the parameters is not robust to outliers. A robust M–type estimates can be obtained by the following procedure:

1. Compute the ML estimates of $\boldsymbol{\theta}$ and obtain a robust scale estimate by replacing (15) by the median absolute deviation of the standardized innovations:

$$\left[\text{med}\left(|u_{it} - \text{med}(u_{it})|\right)/0.6745\right]^2,$$

   where med$(\cdot)$ is the median of the distribution.

2. Run the robust AKF of Section 3 to obtain a clean series.

3. Estimate the parameters on the clean series by ML.

Steps 2–3 may be iterated until the robust AKF coincides with the AKF and no further corrections to the series are made.

3.2 Influence function

The influence function is an essential building block of the robust AKF. In our applications, we shall use the Huber influence function which, for a variable u, is given by

$$\psi(u) = \begin{cases} u, & \text{if} \quad |u| \leq c \\ d = c \ \text{sign}(u), & \text{if} \quad |u| > c \end{cases}$$

The Huber function belongs to the class of monotone non–decreasing influence functions and is the most–widely used influence function. The tuning constant c regulates the trade–off between the so–called breakdown point and the efficiency of the estimator. The breakdown point is a measure of robustness of an estimator as it gives the fraction of bad data the estimator can tolerate before giving results towards the boundary of the parameter space. Lower values of c increase the breakdown point but reduce efficiency. We set $c = 1.345$ which guarantees 95% efficiency when sampling from the normal distribution. The Huber influence function $\psi(u)$ and the corresponding weight function $w(u) = \psi(u)/u$ for $c = 1.345$ are depicted in Figure 1.

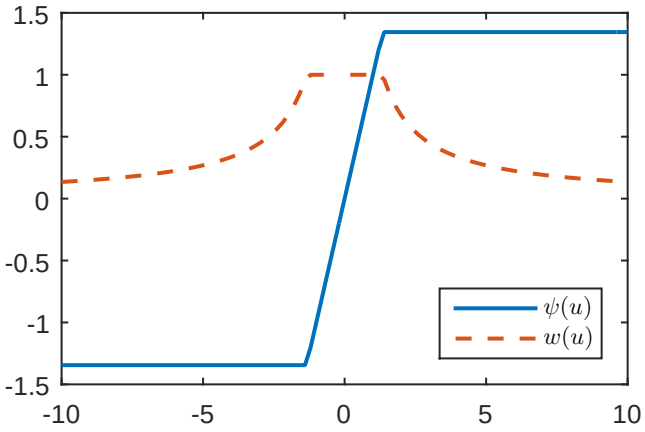

Figure 1: Huber influence function $\psi(u)$ and weight function $w(u)$ for $c = 1.345$.

4 Modeling Framework: the Basic Structural Model

After the robust AKF has been introduced for a general class of linear Markovian models, in the following we review the BSM, which will serve as the common modeling framework in the application part of the article.

The BSM postulates an additive and orthogonal decomposition of a time series into unobserved components representing the trend, seasonality and the irregular component. If y_t denotes a time series observed at $t = 1, \ldots, n$, the decomposition can be written as follows:

$$y_t = \mu_t + \gamma_t + \epsilon_t, \quad t = 1, \ldots, n, \tag{17}$$

where μ_t is the trend component, γ_t is the seasonal component, and $\epsilon_t \sim$ IID $\mathrm{N}(0, \sigma_\epsilon^2)$ is the irregular component.[1]

The trend component has a local linear representation:

$$\begin{array}{rcll} \mu_{t+1} & = & \mu_t + & \rho_t + \eta_t \\ \rho_{t+1} & = & & \rho_t + \zeta_t, \end{array} \tag{18}$$

where η_t and ζ_t are mutually and serially uncorrelated normally distributed random shocks with zero mean and variances σ_η^2 and σ_ζ^2, respectively.

The seasonal component can be modeled as a combination of six stochastic cycles whose common variance is σ_ω^2. The single stochastic cycles have a trigonometric representation and are defined at the seasonal frequencies $\lambda_j = 2\pi j/12$, $j = 1, \ldots, 6$. The parameter λ_1 denotes the fundamental frequency (corresponding to a period of 12 monthly observations) and the remaining ones represent the five harmonics (corresponding to periods of 6 months, i.e. two cycles in a year, 4 months, i.e. three cycles in a year, 3 months, i.e. four cycles in a year, 2.4, i.e. five cycles in a year, and 2 months):

$$\gamma_t = \sum_{j=1}^{6} \gamma_{jt}, \qquad \begin{bmatrix} \gamma_{j,t+1} \\ \gamma_{j,t+1}^* \end{bmatrix} = \begin{bmatrix} \cos\lambda_j & \sin\lambda_j \\ -\sin\lambda_j & \cos\lambda_j \end{bmatrix} \begin{bmatrix} \gamma_{j,t} \\ \gamma_{j,t}^* \end{bmatrix} + \begin{bmatrix} \omega_{j,t} \\ \omega_{j,t}^* \end{bmatrix}, j = 1, \ldots, 5, \tag{19}$$

and $\gamma_{6,t+1} = -\gamma_{6t} + \omega_{6t}$. The disturbances ω_{jt} and ω_{jt}^* are normally and independently distributed with common variance σ_ω^2 for $j = 1, \ldots, 5$, whereas $\mathrm{Var}(\omega_{6t}) = 0.5\sigma_\omega^2$.

The state space representation (1) of the BSM has $m = 13$ state components, $\boldsymbol{\alpha}_t = [\mu_t, \rho_t, \gamma_{1t}, \gamma_{1t}^*, \ldots, \gamma_{6t}]'$, and disturbances

$$\boldsymbol{\varepsilon}_t = \sigma \left[\frac{\epsilon_t}{\sigma_\epsilon}, \frac{\eta_t}{\sigma_\eta}, \frac{\zeta}{\sigma_\zeta}, \frac{\omega_{1t}}{\sigma_\omega}, \ldots, \frac{\omega_{6t}}{\sigma_\omega} \right]'.$$

The system matrices are time–invariant, $\mathbf{Z}_t = \mathbf{Z}, \mathbf{G}_t = \mathbf{G}, \mathbf{T}_t = \mathbf{T}, \mathbf{H}_t = \mathbf{H}$, and

$$\mathbf{Z} = [1, 0, 1, 0, \ldots, 1], \mathbf{G} = \left[\frac{\sigma_\epsilon}{\sigma}, 0, \ldots, 0 \right],$$

[1] Eq. (17) can additionally include regressors that account for any known interventions as well as calendar effects which are, apart from outlier effects, typically also removed during seasonal adjustment.

$$\mathbf{T} = \begin{bmatrix} 1 & 1 & 0 & 0 & \dots & \dots & 0 \\ 0 & 1 & 0 & 0 & \dots & \dots & 0 \\ 0 & 0 & \cos\lambda 1 & \sin\lambda_1 & \dots & \dots & 0 \\ 0 & 0 & -\sin\lambda 1 & \cos\lambda_1 & \dots & \dots & 0 \\ \vdots & \vdots & \dots & \dots & \ddots & \ddots & \vdots \\ 0 & 0 & 0 & 0 & \dots & \dots & -1 \end{bmatrix}, \mathbf{H} = \frac{1}{\sigma} \begin{bmatrix} 0 & \sigma_\eta & 0 & 0 & \dots & \dots & 0 \\ 0 & 0 & \sigma_\omega & 0 & \dots & \dots & 0 \\ 0 & 0 & 0 & \sigma_\omega & \dots & \dots & 0 \\ 0 & 0 & 0 & 0 & \ddots & \dots & 0 \\ \vdots & \vdots & \dots & \dots & \ddots & \ddots & \vdots \\ 0 & 0 & 0 & 0 & \dots & \dots & \sqrt{0.5}\sigma_\omega \end{bmatrix}.$$

Moreover, it holds that $\mathbf{W}_t = \mathbf{0}$, $t = 1, \dots, n$. The scale parameter σ^2 is set equal to one of the variance parameters, and we adopt $\sigma^2 = \sigma_\epsilon^2$ as a default. The initial conditions are set as follows: $\tilde{\boldsymbol{\alpha}}^*_{1|0} = \mathbf{0}$, $\tilde{\boldsymbol{\alpha}}_{1|0} = \boldsymbol{\beta} = \boldsymbol{\alpha}_0^\dagger$, $\mathbf{W}_0 = \mathbf{T}^\dagger$, $\mathbf{T}^\dagger = \mathbf{T}$, and $\mathbf{H}_0 = \mathbf{H}$.

In the next two sections, we illustrate an application of the robust AKF to structural time series models using the BSM. First, in Section 5, we conduct a Monte Carlo experiment to assess the gains in the precision of the parameter estimates when additive or innovation outliers are present in the simulated data. As detection of outliers of this kind may also have consequences for forecasting, in the second step, in Section 6, we illustrate an application of the robust AKF in the context of forecasting. For this purpose, we use a large set of real data contaminated by outliers.

5 A Monte Carlo Experiment

5.1 Design of the experiment

We generate time series of length $n = 144$ observations (12 years of monthly data) using the data generating process (DGP) given by the BSM in eq. (19).[2] We distinguish between five scenarios regarding variance parameters regulating the DGP:

- the benchmark scenario with $\sigma_\epsilon^2 = 1, \sigma_\eta^2 = 0.08, \sigma_\zeta^2 = 0.0001, \sigma_\omega^2 = 0.05$. As the irregular variance is set equal to 1, the remaining parameters are interpreted as signal to noise ratios. The benchmark DGP is chosen on the basis of our experience in fitting the BSM to industrial production and turnover time series. Note that the values of σ_ϵ^2 and σ_ζ^2 remain unchanged across different scenarios.

- a stable trend–stable seasonal scenario (labeled sT–sS) with $\sigma_\eta^2 = 0.00008$ and $\sigma_\omega^2 = 0.00005$

- a stable trend–unstable seasonal scenario (sT–uS) with $\sigma_\eta^2 = 0.00008$ and $\sigma_\omega^2 = 0.5$

[2]The initial values for the components are: $\mu_0 = 91.06$, $\rho_0 = 0.00015$, $[\gamma_{1,0}, \gamma^*_{1,0}] = [-0.381; 4.1483]$, $[\gamma_{2,0}; \gamma^*_{2,0}] = [-6.863; -4.00136]$, $[\gamma_{3,0}; \gamma^*_{3,0}] = [-3.41264; 9.99139]$, $[\gamma_{4,0}; \gamma^*_{4,0}] = [2.032516; -5.47096]$, $[\gamma_{5,0}; \gamma^*_{5,0}] = [-6.65170; 2.93962]$, $\gamma_{6,0} = 5.88545$. These values correspond to the values of the respective smoothed components of the Italian industrial production series in 1995.

- an unstable trend–stable seasonal scenario (uT–sS) with $\sigma_\eta^2 = 0.8$ and $\sigma_\omega^2 = 0.00005$
- an unstable trend–unstable seasonal scenario (uT–uS) with $\sigma_\eta^2 = 0.8$ and $\sigma_\omega^2 = 0.5$

The simulated series are contaminated with randomly located and sized outliers of a particular type. The considered outlier types are: additive outliers (AOs), occurring either individually or in a patch, and innovation outliers (IOs). As a result of outlier contamination, we observe $y_t = y_t^\ddagger + \xi_t$, where $y_t^\ddagger$ is generated according to the BSM and ξ_t represents the outlier effect depending on the outlier type.

The AO generating model is $z_t\,\delta\,I_t$, where δ denotes the reference size, z_t is IID N(0,1), and I_t is an IID Bernoulli random variable with success probability $p = 0.02$. The value of δ and consequences of a random z_t will be discussed later. As for the patch of AOs, we allow only for a single patch of k consecutive outliers, with the first one located at a random time τ. More specifically, we draw k from a discrete uniform distribution with support $\{3, 4, \ldots, 12\}$; the location τ is drawn at random from a uniform distribution with support $\{1, 2, \ldots, n-k+1\}$; setting $I_t(\tau, k) = 1$ for $t = \tau, \ldots, \tau+k-1$, the AO patch is generated by $z_t\,\delta\,I_t(\tau, k)$. In the case of individual AOs, it holds that $\xi_t = \delta z_t I_t$ and for a patch of AOs ξ_t is given by $\xi_t = \delta z_t I_t(\tau, k)$. This means that the outlier signature, i.e. the influence of an outlier occurring at a particular time point on the current and future observations, coincides in both AO cases with the outlier magnitude $z_t\delta$.

In the IO case, for the location τ at which the outlier occurs, we define the dummy variable taking values

$$D_t(\tau) = \begin{cases} 0, & t = 1, \ldots, \tau - 1 \\ 1, & t = \tau \\ \mathbf{Z}\mathbf{T}^{t-\tau-1}\mathbf{K}^*, & t = \tau + 1, \ldots, n, \end{cases}$$

where $\mathbf{K}^*$ denotes the Kalman gain in the steady state. The outlier signature is thus given by the impulse–response function derived from the innovation form of the state space model (1). The occurrence of outliers is, similarly as in the AO case, governed by an IID Bernoulli random variable I_t with success probability $p = 0.02$. If $I_t = 1$ at locations $t = \tau_j, j = 1, \ldots, J$, then the outlier effect at each time point t is given by $\xi_t = \sum_{j=1}^{J} z_j\,\delta\,D_t(\tau_j)$, where z_j are IID standard normal draws.

The reference size δ is expressed by $\delta = 7{\cdot}\text{PESD}$ with $\text{PESD} = \sigma F^{1/2}$ denoting the prediction error standard deviation, which is obtained from the innovations form of the model in the steady state ($F = \lim_{t\to\infty} F_t$). The PESD increases with σ_η^2 and σ_ω^2 and attains the highest value in the uT–uS scenario. Hence, tying δ to the PESD accounts for the difficulty of detecting outliers in the case of a high overall variation. A detailed discussion of the choice of the outlier magnitude for structural time series models is

provided by Marczak and Proietti (2015), who consider the same settings regarding the model for simulations (BSM) and the values for the variance parameters. In addition to the reference size $\delta = 7 \cdot \text{PESD}$, also chosen as a reference size in Marczak and Proietti (2015), we consider $\delta = 14 \cdot \text{PESD}$. Increasing the magnitude of δ is motivated by the fact that, in contrast to Marczak and Proietti (2015), the final outlier size is not given by δ but is obtained by scaling δ with a standard normal variable z_t. Since the probability that z_t takes on values between -1 and 1 is 68.27%, the final outlier size is in most of the cases smaller than δ. A higher δ is thus supposed to countervail low values of z_t. It is to be noted that instead of scaling δ with a random number, we could have examined different values of δ obtained by scaling PESD with a range of factors. However, our setting is a more realistic one as it allows for different sizes of outliers affecting a particular series whereas the alternative setting would imply the same deterministic magnitude.

Taking into account the settings described above, for each combination of the variance parameters and outlier types a simulation experiment is conducted to evaluate the performance of the robust AKF. Every single experiment consists of the following steps:[3]

1. Obtain series contaminated with outliers using the BSM and an outlier generating process.

2. Fit the simulated series to the BSM and put the BSM into the state space form (1).

3. Run the ordinary AKF to the simulated series and the state space model and, by maximizing the likelihood function in eq. (16), obtain the ML estimates of the variance parameters: $\hat{\sigma}_\epsilon^2, \hat{\sigma}_\eta^2, \hat{\sigma}_\zeta^2, \hat{\sigma}_\omega^2$.

4. Apply the procedure described in Section 3.1 to obtain the robust estimates of the parameters: $\tilde{\sigma}_\epsilon^2, \tilde{\sigma}_\eta^2, \tilde{\sigma}_\zeta^2, \tilde{\sigma}_\omega^2$.

5. After 1000 replications of steps 1–4, compute relative efficiency corresponding to each of the variance parameters, given by the ratio of the mean square error (MSE) of the ML estimates to the MSE of the robust estimates.

[3]All computations are performed with Matlab R2015a. We also experimented with different values of δ and, as alternatives to the Huber function, we also investigated different redescending functions, which exhibit higher resistance to large outliers than monotone functions. More specifically, we considered the Chauchy function as a soft redescender and two strong redescenders – the Hampel function and the Tukey biweight function. The latter two proved inferior to the Huber function in the Monte Carlo experiment. The Cauchy function yielded, similarly to the Huber function, satisfactory results but at the cost of overadjusting the series. These further outcomes of the simulation experiment are available from the authors upon request.

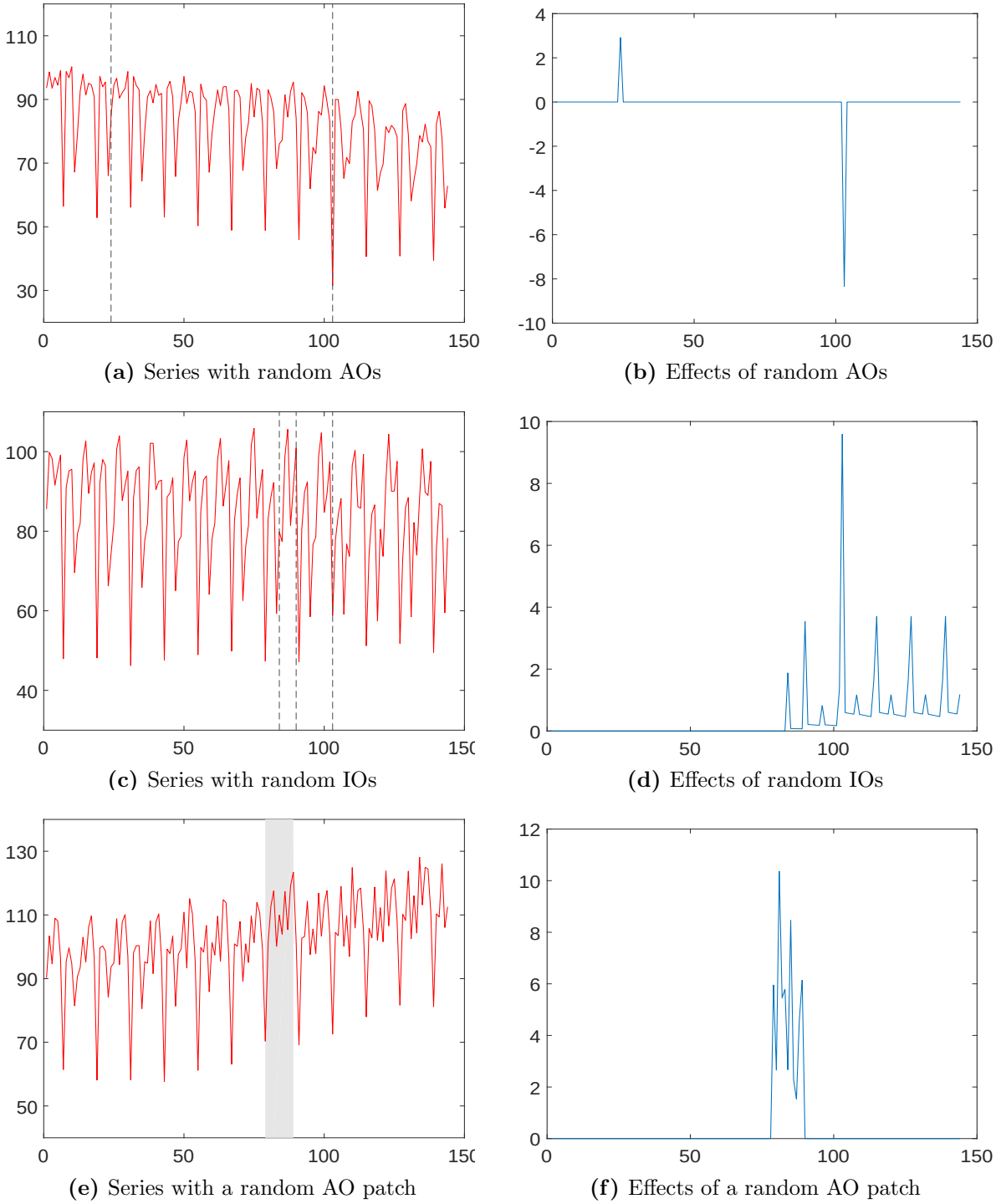

(a) Series with random AOs

(b) Effects of random AOs

(c) Series with random IOs

(d) Effects of random IOs

(e) Series with a random AO patch

(f) Effects of a random AO patch

Figure 2: Examples of simulated series affected by random AOs, IOs, and a random AO patch, respectively (left panel). Location of random outliers of a particular type is indicated by: vertical dashed lines in a) (AOs) and c) (IOs), and a shaded vertical band in e) (AO patch). The corresponding outlier effects are depicted in the right panel. The contaminated series are generated using the benchmark setting; the outlier size is set relative to $\delta = 7 \cdot$ PESD.

5.2 Results

Table 1 summarizes the simulation results for series contaminated by AOs for the five different parameter scenarios outlined above, and two different values of δ regulating the outlier size. In particular, the table displays the relative efficiency of the ML estimator compared to that of the robust estimator of the variance parameters, as measured by the ratio of the respective MSE values. It is evident that for all parameters as well as both values of δ and all variance combinations, the robust estimator is more efficient than the ML estimator. Only for the seasonal variance, σ_ω^2, the efficiency ratio is in one of the ten considered cases slightly below one. Increasing the reference size from the benchmark value to 14·PESD leads, however, to a considerable improvement of the results for all variance parameters. Independently of δ, the most sizeable efficiency gain for the

Table 1: Series contaminated by random AOs: MSE ratio of the ML estimator to that of the robust estimator.

	Benchmark: $\delta = 7$·PESD					$\delta = 14$·PESD				
	Benchmark	sT–sS	uT–sS	sT–uS	uT–uS	Benchmark	sT–sS	uT–sS	sT–uS	uT–uS
σ_ϵ^2	3.695	9.012	6.769	2.532	3.517	5.305	27.022	10.352	5.708	6.459
σ_η^2	1.783	3.536	6.515	5.177	1.380	2.653	10.621	20.823	8.077	6.723
σ_ζ^2	2.145	1.189	3.427	2.930	2.598	2.672	1.290	6.819	2.738	3.507
σ_ω^2	1.675	7.370	3.917	3.302	0.842	4.087	26.199	7.373	7.806	3.001

irregular variance, σ_ϵ^2, is visible in the sT–sS scenario. The gain decreases if the seasonal component is unstable. As regards the variances of the level and the slope disturbance, σ_η^2 and σ_ζ^2, respectively, the efficiency of the robust estimator is the highest in the uT–sS scenario. For σ_ω^2, similarly as for σ_ϵ^2, the robust estimator shows the highest accuracy in the sT–sS case. In general, it can be concluded that the highest accuracy of the robust estimator is achieved if the seasonal component is stable which means that in such a case it is easier to decouple the effect of outliers from the variation of a particular component.

Evaluation results for a random patch of AOs are reported in Table 2. Similarly as for individually occurring AOs, the robust estimator is in general more efficient than the ML estimator, especially if the reference size δ is doubled. For σ_ω^2, the robust estimator turns out to be less efficient if δ is of the benchmark size and the seasonal component is not stable but it improves in efficiency relative to the ML estimator if the reference size is larger. Overall, the efficiency gains are found to be the highest if the seasonal component is stable, with an exception for σ_ζ^2. In this case, the best performance of the robust estimator is observed in the uT–uS and sT–uS scenarios.

If the series are contaminated with random IOs (see Table 3), the general tendency in

Table 2: Series contaminated by a random patch of AOs: MSE ratio of the ML estimator to that of the robust estimator.

	Benchmark: $\delta = 7$·PESD					$\delta = 14$·PESD				
	Benchmark	sT–sS	uT–sS	sT–uS	uT–uS	Benchmark	sT–sS	uT–sS	sT–uS	uT–uS
σ_ϵ^2	4.934	6.147	7.994	4.054	4.741	8.654	17.677	14.863	8.745	9.511
σ_η^2	3.001	4.413	8.243	2.995	3.689	4.009	11.341	16.492	4.736	5.609
σ_ζ^2	3.002	3.446	3.288	2.554	4.134	3.687	8.000	0.966	13.359	4.689
σ_ω^2	0.702	11.097	6.723	0.473	0.461	1.623	22.690	21.537	1.150	1.446

the findings is similar to that for individual AOs and AO patch. For both reference sizes, the highest gain of applying the robust estimator is found for σ_ϵ^2 as well as σ_ω^2 in the sT–sS scenario. For σ_η^2, the robust estimator performs better in terms of efficiency in the uT–sS scenario, like for the previously discussed outlier types. Differently than in the additive outlier case, the efficiency gain is on average the highest for σ_ω^2, a result being especially in contrast to the case of a random AO patch. This difference can be explained by the fact that AOs particularly corrupt the ML estimate of the irregular variance and an AO patch, which resembles a level shift, possibly also distorts the level variance estimate. IOs, on the other hand, affect all components and the distortion is here especially articulate for the ML estimates of the seasonal component.

Table 3: Series contaminated by random IOs: MSE ratio of the ML estimator to that of the robust estimator.

	Benchmark: $\delta = 7$·PESD					$\delta = 14$·PESD				
	Benchmark	sT–sS	uT–sS	sT–uS	uT–uS	Benchmark	sT–sS	uT–sS	sT–uS	uT–uS
σ_ϵ^2	4.476	12.619	4.384	1.504	2.833	6.782	45.443	15.312	2.198	6.124
σ_η^2	1.908	3.559	8.411	2.644	3.933	3.591	19.688	24.039	4.850	8.865
σ_ζ^2	2.107	1.282	2.769	4.230	2.948	2.668	2.253	5.819	2.364	6.515
σ_ω^2	2.026	12.711	4.581	6.803	7.688	4.513	53.330	19.332	6.039	14.750

Next, we compare the distributions of the ML and robust estimates of the BSM parameters is presented in Figure 3 for the benchmark scenario. The plot is divided into three panels, according to the outlier type (AOs, AO patch and IOs). The light blue bars (histogram) and the dashed red line (density) correspond to the ML estimates, whereas the dark blue bars (histogram) and the solid red line (density) refer to the robust estimates.

It can be observed that for all three types of outlier contamination the distribution of the ML estimates of all variance parameters is more dispersed than the distribution of the robust estimates. Further, for all variance parameters, except for σ_ζ^2, the distribution of the ML estimates is shifted to the right relative to that of the robust estimates.

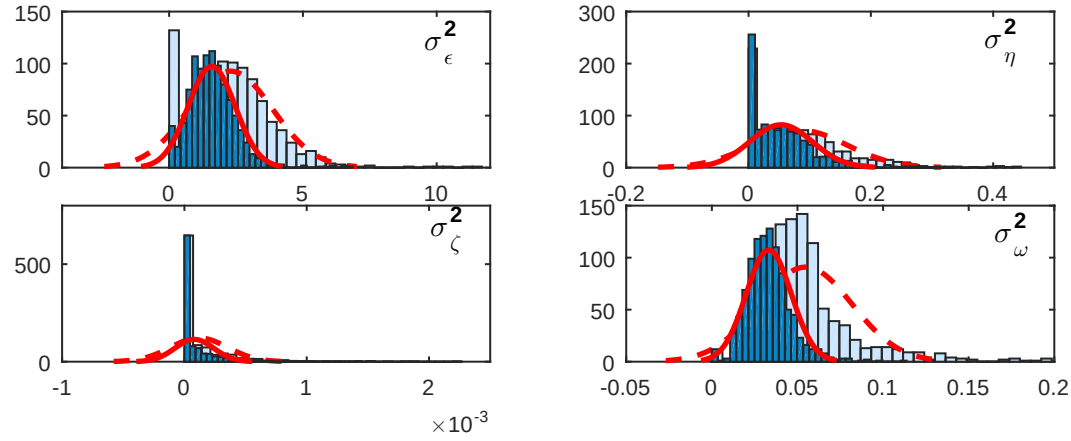

(a) AO

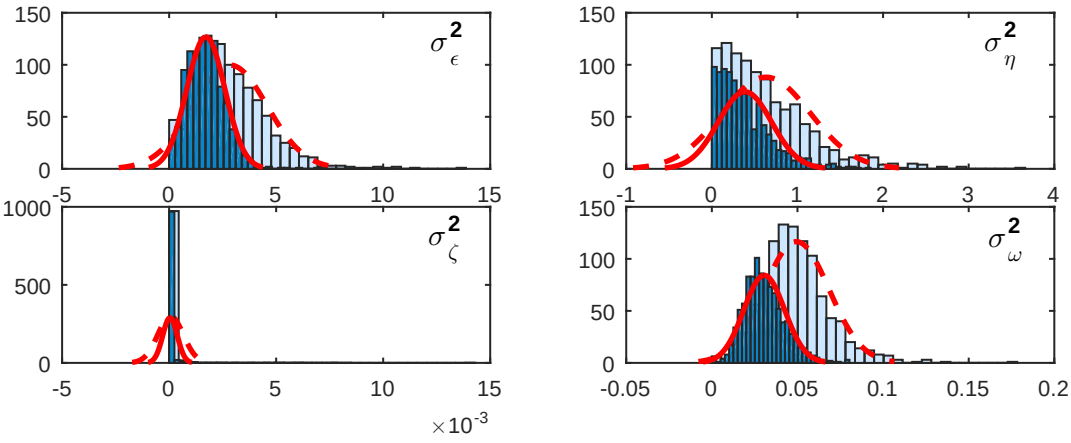

(b) AO patch

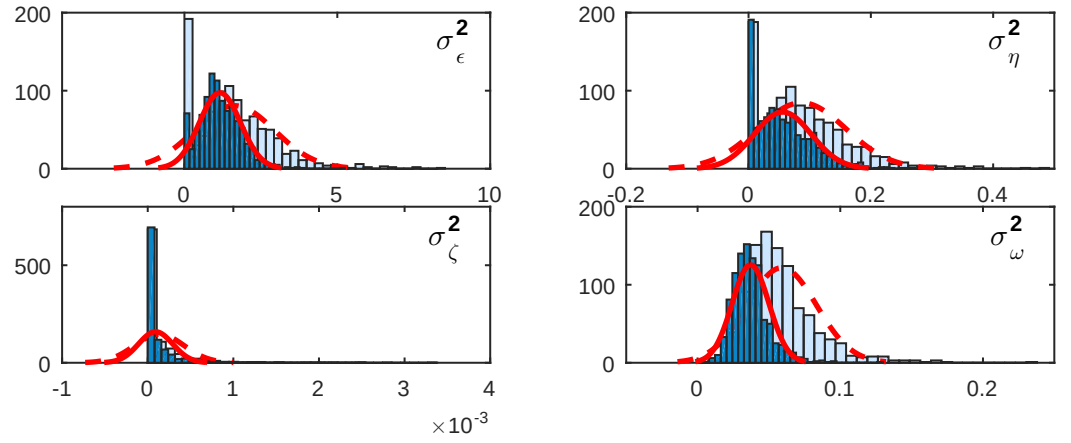

(c) IO

Figure 3: Distribution of the ML and robust estimates of the disturbance variances in the case of individual random AOs, a random patch of AOs and random IOs; ML estimates: light blue bars (histogram) and dashed red line (density), robust estimates: dark blue bars (histogram) and solid red line (density). The true parameter values correspond to the benchmark case: $\sigma^2_\epsilon = 1$, $\sigma^2_\eta = 0.08$, $\sigma^2_\zeta = 0.0001$, $\sigma^2_\omega = 0.05$.

In the case of random AOs (Figure 3a), lower dispersion of the robust estimates is particularly clear for σ_ϵ^2 and σ_ω^2. In addition, the distribution of the robust estimates of σ_ϵ^2 is concentrated around the true value 1. For σ_ω^2, the mode of the distribution in the robust case occurs, in contrast to the ML case, at a value lower than the true one (0.05). However, from the inspection of the histogram it is evident that ML substantially overestimates σ_ω^2 in a large number of cases.

Similar observations as for individual AOs can be made also for a random AO patch and random IOs as regards both parameters, σ_ϵ^2 and σ_ω^2. Unlike in the AO case, for the other outlier types noticeable differences in the distributions of the robust and ML estimates are found also for the parameter σ_η^2. Even though in the case of an AO patch (Figure 3b) both distributions are concentrated around a value distant from the the true one (0.08), ML leads to a considerably larger overestimation of σ_η^2. As the effect of outliers occurring in a group resembles that of a level shift, variance of the level disturbance is estimated by ML with a large positive bias. The robust method thus helps reduce this bias but it is clear that the difficulty of the robust estimator to classify an AO patch as bad observations is bigger than for single random AOs. As far as IOs are concerned (Figure 3c), the distribution of the ML estimates of σ_η^2 peaks around the true value. However, the histogram indicates that ML overestimates σ_η^2 more often than the robust estimator.

Finally, the performance of the robust AKF in detecting outliers is examined. To that end, we compute the proportion of correctly adjusted outliers and focus thereby on individual AOs.[4] The results corresponding to our experiment design with randomly located and sized outliers are reported in Table 4. The findings show that regardless of the scenario and the reference size of the outliers, the robust AKF is capable of identifying AOs in nearly 100% cases. It is thus a very effective outlier detection method.

[4]We restrict the analysis to individual AOs for the following reasons. As regards AO patches, it is well–known that their effect on the series is very similar to that of a level shift lasting for a limited period. Detecting a level shift by capturing the single outlying observations in the time interval of the shift is very difficult; see, e.g., Marczak and Proietti (2015). Therefore, the proportion of identified AOs in a patch is expected to be lower than the proportion of identified single AOs. As regards IOs, differently than for the AO type, the proportion of the correctly adjusted outlier effects may not be an appropriate measure to evaluate an outlier detection method. While the effect of an AO lasts for one period only, the effect of an IO persists until the end of the series. Even though the effect of an IO at the time point of its occurrence would correspond to the effect of an AO, the effects at the subsequent time points may be very small and hardly detectable.

Table 4: Proportion of correctly adjusted outlier effects (in %) in the case of randomly located AOs. The outlier size at a location τ is given by $z_t\,\delta$.

Reference size	Benchmark	sT–sS	uT–sS	sT–uS	uT–uS
Benchmark $\delta = 7{\cdot}$PESD	96.14	99.62	99.45	99.13	99.26
$\delta = 14{\cdot}$PESD	99.96	99.92	99.96	99.96	99.92

6 Robust Forecasting: an Application

If the series is generated as $y_t = y_t^{\ddagger} + \xi_t$, with $y_t^{\ddagger}$ and ξ_t denoting uncontaminated latent series and outlier effects, respectively, robust forecasting deals with predicting $y_t^{\ddagger}$ using the observed past values of y_t. Two issues are involved: the first one is robust estimation of the model parameters; the second one deals with robustifying the forecasting method, so that a contaminated observation does not exert excessive influence on the forecast. Replacing y_t by an estimate of $y_t^{\ddagger}$ in the expression of the optimal linear predictor goes in this direction. The forecast application presented in this section aims at assessing the effectiveness of this strategy for forecasting a set of time series of trade flows. The perspective that is taken here is that we either believe that the outliers are not going to affect the future of y_t, or that we are inherently interested in forecasting the component $y_t^{\ddagger}$. If interest lies in predicting y_t, taking into account that outlier contamination can occur also in the future, so that the predictive density reflects the additional uncertainty due the presence of the outliers, other methods, such as modeling the distribution of the BSM disturbances as scale mixtures of normals, should be applied; see Bruce and Jurke (1996) and Bernardi et al. (2011).

6.1 Data

In the forecasting part of the study, we use a large set of international trade data by BEC product group classification for 28 members of the European Union. The dataset is provided by Eurostat (download at: `http://ec.europa.eu/eurostat/web/international-trade/data/database`, label: `ext_st_28msbec`). The data is given on a monthly basis and the original dataset covers the time span 1991.M1 – 2015.M5. We construct a dataset relevant for our application by taking a subset of the first 560 series. All series from this subset represent trade balance (indicated by the acronym `BAL_RT`) and are non–seasonally adjusted volume indices (`IVOL_NSA`). These series, all related to a respective country of the European Union, are divided into two categories. The first one is the trade partner: euro area without Latvia and Lithuania (`EA17`), euro area without

Lithuania (EA18), euro area with all current members (EA19), or European Union (EU28). The second category is related to the product type: capital goods (CAP), consumption goods (CNS), consumption goods plus motor spirit and passenger motor cars (CTR), or all products (TOTAL). We restrict the sample to the time span 2000.M1 – 2014.M1, as the series for all countries except Croatia are available in this time interval. Non–missing observations for all Croatian series start only in 2003.M1 and thus series corresponding to Croatia are excluded from the analysis. The final dataset consists of 540 series, each having 180 observations.

There are various reasons for considering international trade statistics for the purpose of this article. First, these series are typically contaminated by outliers which, at times, can be large. To illustrate the degree of contamination, four series taken from the dataset are plotted in Figure 4. Second, the dataset has large dimensions – a total of 45,361 series included in the original dataset. Outlier detection in such a case necessitates a procedure which allows for quick processing of each series. Although we focus on a subset of data for illustration purposes, our proposed method provides a simple and fast procedure for robust estimation and forecasting, and is capable of handling big data, like trade statistics. Finally, resorting to a large dataset enables a more reliable evaluation of the proposed data–cleaning procedure.

6.2 Design of the forecasting exercise and results

For the total sample of 540 series, we perform a pseudo real–time recursive forecasting exercise using two specifications. In both cases, each of the series is modeled using the BSM, but in the first one (labeled "non–robust") no correction of the data takes place whereas in the second one (labeled "robust") the robust AKF is applied for data cleaning. Outlier detection and correction in the robust scenario is, just as estimation and predictions, performed in a recursive manner. The training sample covers the time span 2001.M1 – 2009.M1. For a particular series, starting in 2009.M1 as the first forecast origin, we compute 1– to 12–period–ahead non–robust and robust forecasts. Then, for each next forecast origin until 2013.M12, the sample is extended by one month and 1– to 12–period–ahead forecasts are obtained for both specifications. This forecasting exercise yields for each forecast horizon from 1 to 12 a total of 540 forecasts for 60 time points from the respective time span. For example, 1–step–ahead forecasts are available in the time span 2009.M2 – 2014.M1, while the relevant time span for 12–step–ahead forecast is 2010.M1 – 2014.M12.

In the evaluation of the forecasting precision in the non–robust and robust scenario, we focus on the assessment of the respective forecast densities instead of point forecasts. As

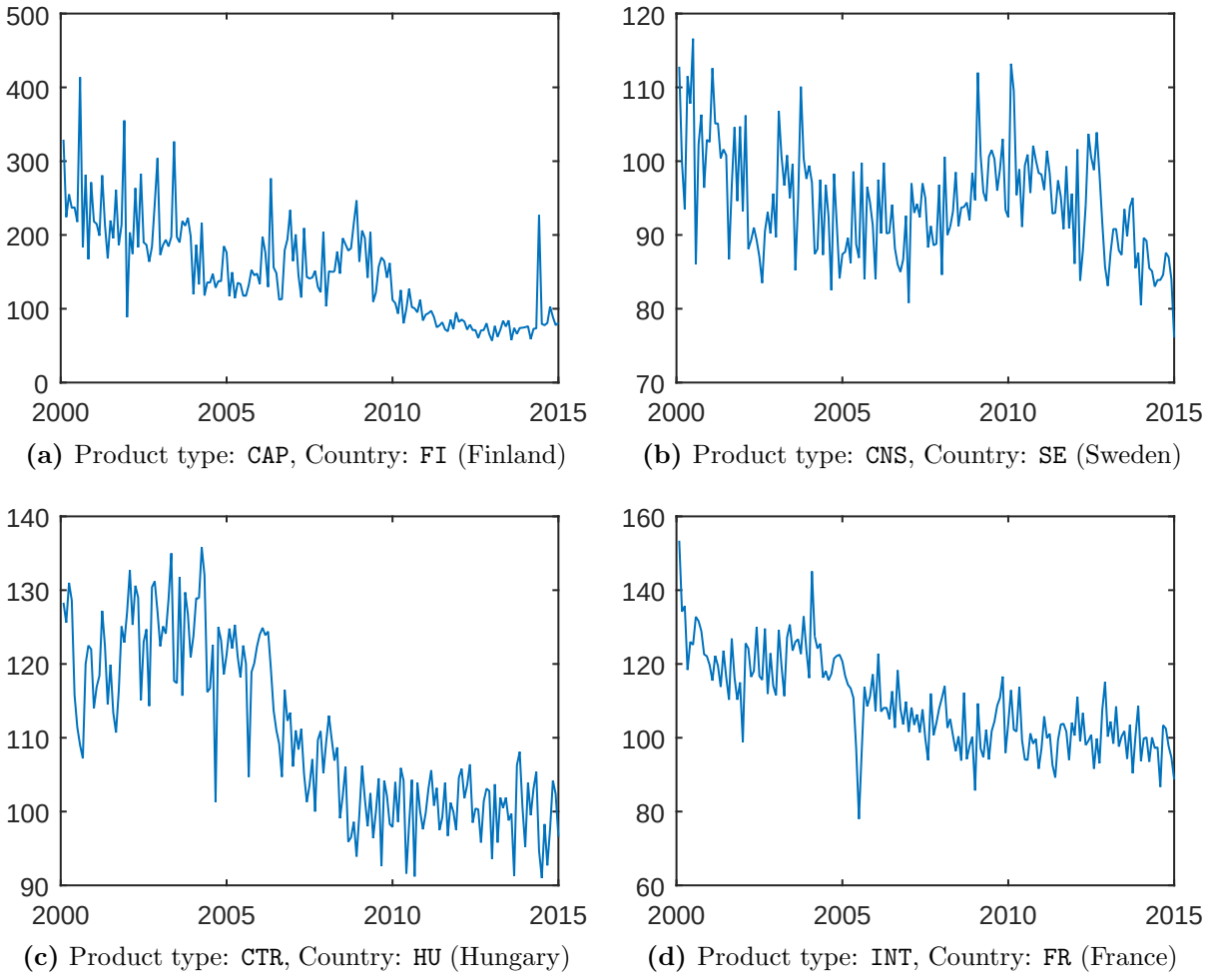

(a) Product type: `CAP`, Country: `FI` (Finland)

(b) Product type: `CNS`, Country: `SE` (Sweden)

(c) Product type: `CTR`, Country: `HU` (Hungary)

(d) Product type: `INT`, Country: `FR` (France)

Figure 4: Four series from the international trade statistics dataset for 28 members of the European Union. Each series depicted in the figure has the signature `BAL_RT,IVOL_NSA,EA17`, belongs to one of four product categories (`CAP`, `CNS`, `CTR`, `INT`), and represents one of 28 European Union countries.

shown by Ledolter (1989) in an ARIMA framework, point forecasts are largely unaffected by additive outliers unless there are very close to the forecast origin. In contrast, outliers always inflate the variance of the prediction errors and, hence, the width of the prediction intervals. This means that even though the location of the forecast densities corresponding to contaminated and clean data may be very similar, the spread of the latter density is supposed to be smaller. The aim of the forecasting exercise is to test whether data cleaning by means of the robust AKF has a beneficial effect on the prediction uncertainty.

Forecast densities associated with each point forecast are in this study obtained conditionally on the estimated parameters and assuming Gaussianity.[5] To compare the sharp-

[5]Giving up the Gaussianity assumption and accounting for parameter uncertainty would on the one

ness of densities associated with non–robust and robust forecasts, we apply scoring rules for evaluating the quality of density forecast. See Gneiting and Raftery (2007) for a comprehensive review of different scoring rules. In this article, we adopt two proper scores: the log score, proposed by Good (1952), and the continuous ranked probability score (CRPS), introduced by Matheson and Winkler (1976).[6] The log score (LogS) at the realized outcome y_t is given as:

$$\mathrm{LogS}(y_t) = \log f(y_t),$$

where $f(u)$ denotes a density forecast with the corresponding cumulative distribution function $F(u)$. Despite the desirable properties of the log score and its widespread use in the evaluation of density forecasts, one drawback is its lack of robustness. For example, in the presence of outliers, if for a single observation the forecast density is completely missing the realized outcome, the log score attached to this observation approaches $-\infty$. As a consequence, if a forecasting model is evaluated based on an average score, then the log scoring rule discredits this model, even if its overall forecasting performance at all other observations might be good. Therefore, to safeguard against the possible non–robustness of the log score, we also adopt the CRPS – a more robust and tolerant scoring rule which assigns high numerical scores for probabilities at values close, but not necessarily equal, to the realized one. CRPS penalizes deviations of the predictive cumulative distribution function from the true one for a particular time point. More formally,

$$\mathrm{CRPS}(y_t) = -\int [F(u) - I(y_t)]^2 \, \mathrm{d}u, \tag{20}$$

where $I(\cdot)$ is an indicator variable taking value 1, if $u > y_t$, and 0 otherwise. Eq. (20) can be also written as (Gneiting and Raftery, 2007):

$$\mathrm{CRPS}(y_t) = \frac{1}{2}\,\mathrm{E}_F|Y - Y'| - \mathrm{E}_F|Y - y_t|, \tag{21}$$

where E_F is the expectation with respect to the forecast distribution F, and Y and Y' are independent random draws from F. For the computation of the CRPS according to eq. (21), we implement algorithms for approximating expressions in eq. (21) provided by

hand provide more reliable forecast densities, on the other hand it would require computationally expensive algorithms, such as bootstrapping. In the case of a large set of series, the computational burden is too high relatively to the gain in terms of more reliable prediction densities. Moreover, our interest lies in the comparison of density forecasts in the non–robust and robust case, and as the densities are obtained based on the same assumptions, the uncertainty will be underestimated in both cases.

[6] A scoring rule is proper if the expected value of the score is maximized for an observation drawn from the distribution being the same as the one the forecasts are issued from.

Panagiotelis and Smith (2008).

To facilitate the comparison between the non–robust and robust forecasts, we consider differences between the score values (log score or CRPS) obtained in the robust and non–robust case. As both the log score and the CRPS are defined in a way that higher values indicate a lower dispersion, positive score differences are in our case an evidence of the superiority of the robust alternative. The forecasting experiment based on the full set of series results, for a particular forecast horizon from 1 to 12, in the distribution of the log score and CRPS differences given at each time point of the evaluation sample. The empirical distributions of the score differences based on 540 series are smoothed using a Gaussian kernel.

The smoothed distributions of differences between scores corresponding to the robust and non–robust forecasts are depicted in Figure 5. The selected forecast horizons are 1, 6 and 12 months. The height of the surface plot at each point as well as the color along with the hue give the information about the probability value. The color scale ranges from dark indicating the lowest probabilities to the yellow indicating the highest probabilities. To make the results easier to interpret, each three–dimensional surface plot is projected on a two–dimensional plane. It is evident that for both scoring rules and all forecast horizons, the mass of the distribution at any of the time points is concentrated at positive values of the score differences. This means that the scores associated with the robust forecasts are higher or, in other words, forecasts obtained with cleaned data are fraught with lower uncertainty. The results in favor of the robust alternative are, independent of the forecast horizon, more pronounced in the CRPS case. As regards the log score, the superiority of the robust alternative is especially visible in the case of 1–period–ahead forecasts.

All these findings confirm that, for the considered set of international trade statistics, the robust AKF effectively cleans the data, which is reflected in the reduced forecast uncertainty and in better calibrated predictive densities.

7 Conclusions

This paper develops a robust augmented Kalman filter (AKF) for data cleaning. This algorithm allows for a robust estimation of model parameters if the data contaminated with outliers is nonstationary and/or the model features regressor effects. The idea for achieving robustness is in our framework based on the correction of an observation classified as a contaminated one towards its one–step–ahead prediction by using an influence function. Our methodology combines the approach of the robust Kalman filter by Masreliez and Martin (1977) with the augmentation approach for the Kalman filter accounting for the

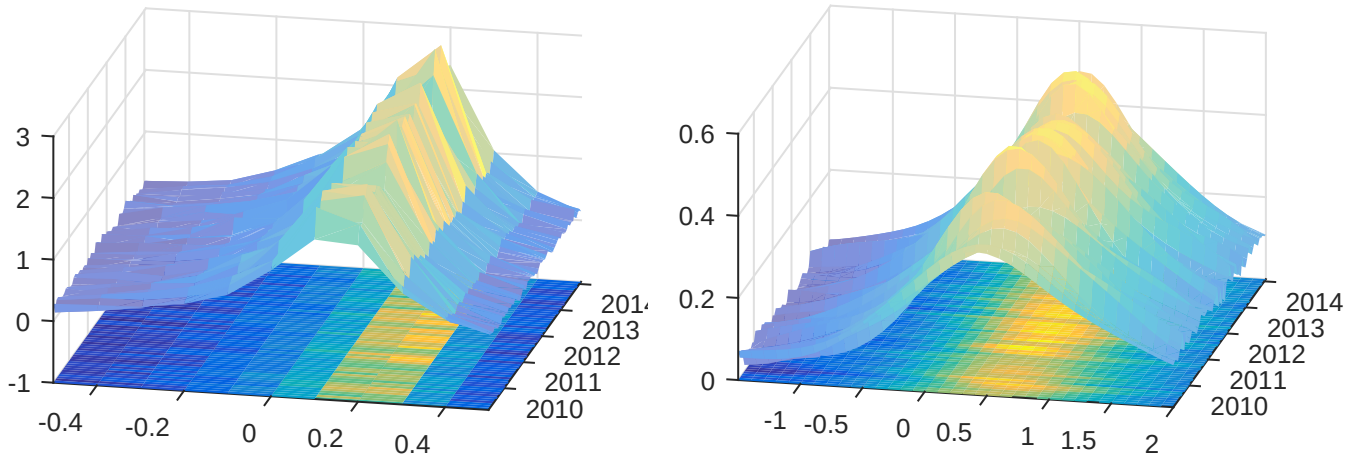

(a) Log score: 1–step–ahead forecasts

(b) CRPS: 1–step–ahead forecasts

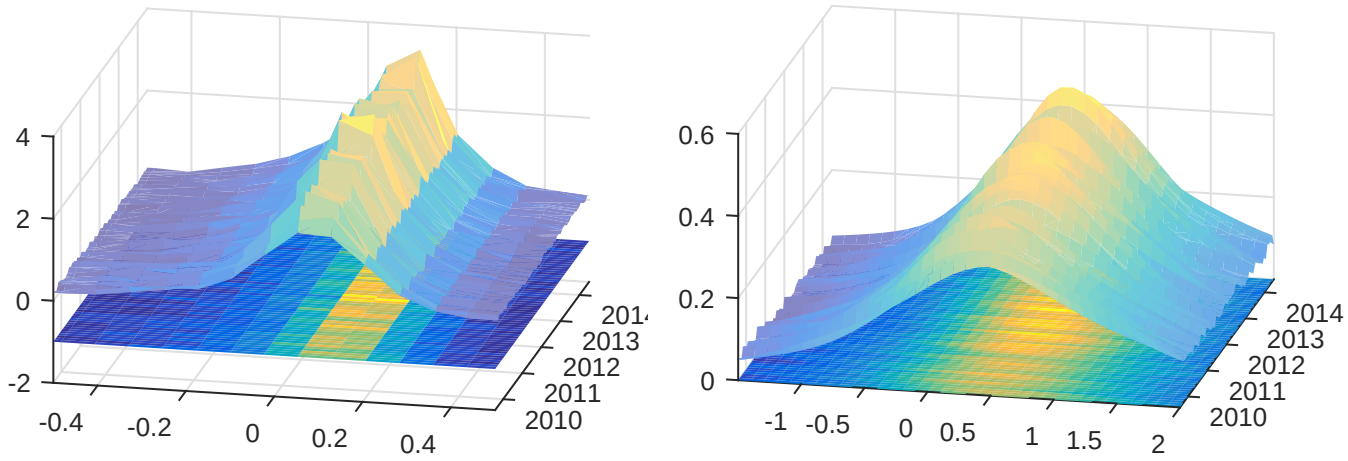

(c) Log score: 6–step–ahead forecasts

(d) CRPS: 6–step–ahead forecasts

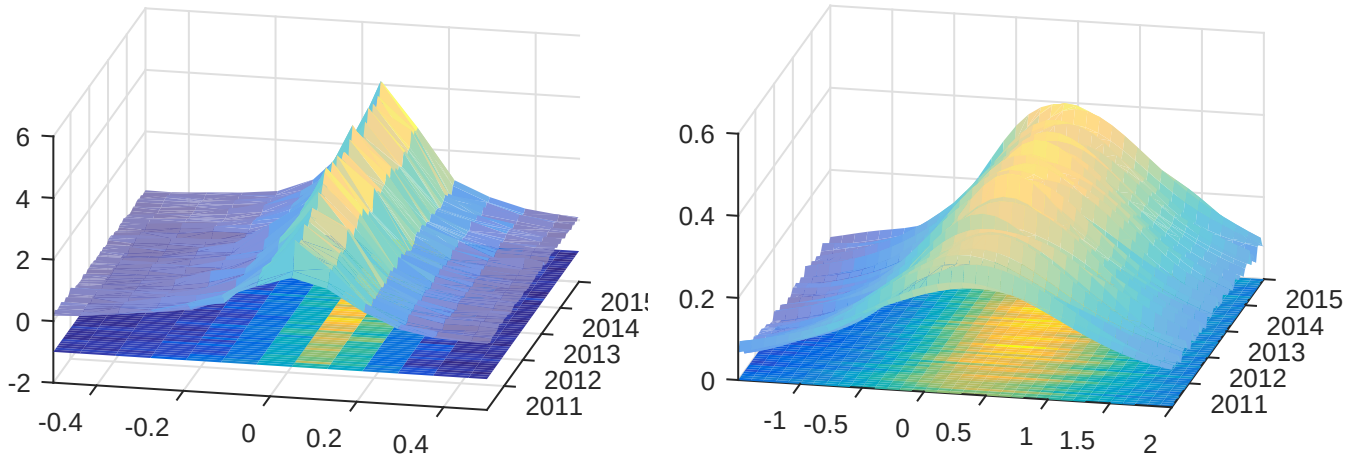

(e) Log score: 12–step–ahead forecasts

(f) CRPS: 12–step–ahead forecasts

Figure 5: Distributions of differences in the scores based on the robust and non–robust forecasts for 540 European trade statistics series. The robust (non–robust) forecasts are obtained in a pseudo real–time recursive forecasting exercise using cleaned (original) data. Data cleaning is performed recursively for each forecast origin. Training sample: 2000.M1 – 2009.M1; evaluation sample: 2009.2 – 2014.M12. Rows indicate the corresponding forecast horizons: (from top to bottom) 1–, 6,–, and 12–step–ahead forecasts. Left panel: log score differences; right panel: CRPS differences. Empirical densities are smoothed using the Gaussian kernel.

presence of nonstationary elements and regressors (de Jong, 1991).

For the purpose of evaluating the proposed method we focus on the class of structural time series models and, in particular, on the basic structural model (BSM) which is a popular model used for seasonal adjustment. In the application part of the paper, we conduct in the first step a Monte Carlo experiment, in which the series generated according to the BSM with different parameter settings are affected by random additive outliers (AOs) occurring either individually or in a patch, and random innovation outliers (IOs).

To assess the performance of the robust AKF, we compare the efficiency of the M–type robust estimator based on the robust AKF relative to the maximum–likelihood (ML) estimator. The results show that for all three types of outlier contamination and for all four disturbance variances the robust estimates are more accurate. The gain in efficiency is, in general, the highest if the seasonal component is stable. Whereas in the case of individual AOs the robust method shows, on average, the highest efficiency for the irregular variance, in the case of random IOs it is the variance of the seasonal disturbance that benefits the most from the application of the robust estimator. After the Monte Carlo experiment, in the next step we apply the robust AKF in the context of a recursive forecasting exercise. The examined dataset is a set of 540 European trade statistics series contaminated with AOs. We compare the dispersion of the forecast density based on the original data with that related to the data cleaned with the robust AKF where the cleaning is performed for every sample changing with the new forecast origin. As measures for the evaluation of the distribution spread, we have applied two scoring rules: the log score and the continuous ranked probability score. The conclusion from this application is that data cleaning with the robust AKF reduces the forecast uncertainty. Our proposed method is thus suitable for cleaning data affected by AOs or IOs. Being a simple and fast procedure, the robust AKF is a particularly attractive tool for handling large sets of series, like the international trade statistics database.

References

Bernardi, M., Della Corte, G., and Proietti, T. (2011). Extracting the Cyclical Component in Hours Worked. *Studies in Nonlinear Dynamics & Econometrics*, *15*(3).

Bianco, A. M., Garcia Ben, M., Martinez, E., and Yohai, V. J. (2001). Outlier Detection in Regression Models with ARIMA Errors Using Robust Estimates. *Journal of Forecasting*, *20*(8), 565–579.

Bruce, A. G., and Jurke, S. R. (1996). Non–Gaussian Seasonal Adjustment: X–12–ARIMA versus Robust Structural Models. *Journal of Forecasting*, *15*(4), 305–327.

de Jong, P. (1991). The Diffuse Kalman Filter. *The Annals of Statistics*, *19*, 1073–1083.

Francke, M. K., Koopman, S. J., and De Vos, A. F. (2010). Likelihood Functions for State Space Models with Diffuse Initial Conditions. *Journal of Time Series Analysis*, *31*(6), 407–414.

Gandhi, M. A., and Mili, L. (2010). Robust Kalman Filter Based on a Generalized Maximum–Likelihood–Type Estimator. *IEEE Transactions on Signal Processing*, *58*(5), 2509–2520.

Gneiting, T., and Raftery, A. E. (2007). Strictly Proper Scoring Rules, Prediction, and Estimation. *Journal of the American Statistical Association*, *102*(477), 359–378.

Good, I. J. (1952). Rational Decisions. *Journal of the Royal Statistical Society: Series B*, *14*(1), 1107–114.

Harvey, A. C. (1989). *Forecasting, Structural Time Series Models and the Kalman Filter.* Cambridge: Cambridge University Press.

Harvey, A. C. (2013). *Dynamic Models for Volatility and Heavy Tails: with Applications to Financial and Economic Time Series* (No. 52). Cambridge University Press.

Harvey, A. C., and Todd, P. H. J. (1983). Forecasting Econometric Time Series with Structural and Box-Jenkins Models (with discussion). *Journal of Business and Economic Statistics*, *1*(4), 299–315.

Henderson, H. V., and Searle, S. R. (1981). On Deriving the Inverse of a Sum of Matrices. *Siam Review*, *23*(1), 53–60.

Ledolter, J. (1989). The Effect of Additive Outliers on the Forecasts from ARIMA Models. *International Journal of Forecasting*, *5*, 231–240.

Liu, H., Shah, S., and Jiang, W. (2004). On–line Outlier Detection and Data Cleaning. *Computers and Chemical Engineering*, *28*, 1635–1647.

Marczak, M., and Proietti, T. (2015). Outlier Detection in Structural Time Series Models: the Indicator Saturation Approach. *International Journal of Forecasting*, *forthcoming*.

Maronna, R., Martin, D., and Yohai, V. (2006). *Robust Statistics*. John Wiley & Sons, Chichester. ISBN.

Martin, R. D. (1979). Robust Estimation for Time Series Autoregressions. In R. L. Launer and G. N. Wilkinson (Eds.), *Robustness in Statistics* (pp. 147–176). New York: Academic Press.

Martin, R. D., and Thomson, D. J. (1982). Robust–resistant Spectrum Estimation. *Proceedings of the IEEE*, *70*, 1097–1115.

Masreliez, C. J., and Martin, R. D. (1977). Robust Bayesian Estimation for the Linear Model and Robustifying the Kalman Filter. *IEEE Transactions on Automatic Control*, *AC–22*, 361–371.

Matheson, J. E., and Winkler, R. L. (1976). Scoring Rules for Continuous Probability Distributions. *Management Science*, *22*(10), 1087–1096.

Panagiotelis, A., and Smith, M. (2008). Bayesian Density Forecasting of Intraday Electricity Prices Using Multivariate Skew t Distributions. *International Journal of Forecasting*, *24*, 710–727.

Rosenberg, B. (1973). Random Coefficients Models: the Analysis of a Cross Section of Time Series by Stochastically Convergent Parameter Regression. In *Annals of Economic and Social Measurement* (Vol. 2, pp. 399–428). NBER.

Ruckdeschel, P., Spangl, B., and Pupashenko, D. (2014). Robust Kalman Tracking and Smoothing with Propagating and Non–propagating Outlier. *Statistical Papers*, *55*, 93–123.

Hohenheim Discussion Papers in Business, Economics and Social Sciences

The Faculty of Business, Economics and Social Sciences continues since 2015 the established “FZID Discussion Paper Series” of the “Centre for Research on Innovation and Services (FZID)” under the name “Hohenheim Discussion Papers in Business, Economics and Social Sciences”.

Institutes

510 Institute of Financial Management
520 Institute of Economics
530 Institute of Health Care & Public Management
540 Institute of Communication Science
550 Institute of Law and Social Sciences
560 Institute of Economic and Business Education
570 Institute of Marketing & Management
580 Institute of Interorganisational Management & Performance

Download Hohenheim Discussion Papers in Business, Economics and Social Sciences
from our homepage: https://wiso.uni-hohenheim.de/papers

Nr.	Autor	Titel	Inst.
01-2015	Thomas Beissinger, Philipp Baudy	THE IMPACT OF TEMPORARY AGENCY WORK ON TRADE UNION WAGE SETTING: A Theoretical Analysis	520
02-2015	Fabian Wahl	PARTICIPATIVE POLITICAL INSTITUTIONS AND CITY DEVELOPMENT 800-1800	520
03-2015	Tommaso Proietti, Martyna Marczak, Gianluigi Mazzi	EuroMInd-D: A DENSITY ESTIMATE OF MONTHLY GROSS DOMESTIC PRODUCT FOR THE EURO AREA	520
04-2015	Thomas Beissinger, Nathalie Chusseau, Joël Hellier	OFFSHORING AND LABOUR MARKET REFORMS: MODELLING THE GERMAN EXPERIENCE	520
05-2015	Matthias Mueller, Kristina Bogner, Tobias Buchmann, Muhamed Kudic	SIMULATING KNOWLEDGE DIFFUSION IN FOUR STRUCTURALLY DISTINCT NETWORKS – AN AGENT-BASED SIMULATION MODEL	520
06-2015	Martyna Marczak, Thomas Beissinger	BIDIRECTIONAL RELATIONSHIP BETWEEN INVESTOR SENTIMENT AND EXCESS RETURNS: NEW EVIDENCE FROM THE WAVELET PERSPECTIVE	520
07-2015	Peng Nie, Galit Nimrod, Alfonso Sousa-Poza	INTERNET USE AND SUBJECTIVE WELL-BEING IN CHINA	530
08-2015	Fabian Wahl	THE LONG SHADOW OF HISTORY ROMAN LEGACY AND ECONOMIC DEVELOPMENT – EVIDENCE FROM THE GERMAN LIMES	520
09-2015	Peng Nie, Alfonso Sousa-Poza	COMMUTE TIME AND SUBJECTIVE WELL-BEING IN URBAN CHINA	530

Nr.	Autor	Titel	Inst.
10-2015	Kristina Bogner	THE EFFECT OF PROJECT FUNDING ON INNOVATIVE PERFORMANCE AN AGENT-BASED SIMULATION MODEL	520
11-2015	Bogang Jun, Tai-Yoo Kim	A NEO-SCHUMPETERIAN PERSPECTIVE ON THE ANALYTICAL MACROECONOMIC FRAMEWORK: THE EXPANDED REPRODUCTION SYSTEM	520
12-2015	Volker Grossmann Aderonke Osikominu Marius Osterfeld	ARE SOCIOCULTURAL FACTORS IMPORTANT FOR STUDYING A SCIENCE UNIVERSITY MAJOR?	520
13-2015	Martyna Marczak Tommaso Proietti Stefano Grassi	A DATA–CLEANING AUGMENTED KALMAN FILTER FOR ROBUST ESTIMATION OF STATE SPACE MODELS	520

FZID Discussion Papers
(published 2009-2014)

Competence Centers

IK	Innovation and Knowledge
ICT	Information Systems and Communication Systems
CRFM	Corporate Finance and Risk Management
HCM	Health Care Management
CM	Communication Management
MM	Marketing Management
ECO	Economics

Download FZID Discussion Papers from our homepage: https://wiso.uni-hohenheim.de/archiv_fzid_papers

Nr.	Autor	Titel	CC
01-2009	Julian P. Christ	NEW ECONOMIC GEOGRAPHY RELOADED: Localized Knowledge Spillovers and the Geography of Innovation	IK
02-2009	André P. Slowak	MARKET FIELD STRUCTURE & DYNAMICS IN INDUSTRIAL AUTOMATION	IK
03-2009	Pier Paolo Saviotti, Andreas Pyka	GENERALIZED BARRIERS TO ENTRY AND ECONOMIC DEVELOPMENT	IK
04-2009	Uwe Focht, Andreas Richter and Jörg Schiller	INTERMEDIATION AND MATCHING IN INSURANCE MARKETS	HCM
05-2009	Julian P. Christ, André P. Slowak	WHY BLU-RAY VS. HD-DVD IS NOT VHS VS. BETAMAX: THE CO-EVOLUTION OF STANDARD-SETTING CONSORTIA	IK
06-2009	Gabriel Felbermayr, Mario Larch and Wolfgang Lechthaler	UNEMPLOYMENT IN AN INTERDEPENDENT WORLD	ECO
07-2009	Steffen Otterbach	MISMATCHES BETWEEN ACTUAL AND PREFERRED WORK TIME: Empirical Evidence of Hours Constraints in 21 Countries	HCM
08-2009	Sven Wydra	PRODUCTION AND EMPLOYMENT IMPACTS OF NEW TECHNOLOGIES – ANALYSIS FOR BIOTECHNOLOGY	IK
09-2009	Ralf Richter, Jochen Streb	CATCHING-UP AND FALLING BEHIND KNOWLEDGE SPILLOVER FROM AMERICAN TO GERMAN MACHINE TOOL MAKERS	IK

Nr.	Autor	Titel	CC
10-2010	Rahel Aichele, Gabriel Felbermayr	KYOTO AND THE CARBON CONTENT OF TRADE	ECO
11-2010	David E. Bloom, Alfonso Sousa-Poza	ECONOMIC CONSEQUENCES OF LOW FERTILITY IN EUROPE	HCM
12-2010	Michael Ahlheim, Oliver Frör	DRINKING AND PROTECTING – A MARKET APPROACH TO THE PRESERVATION OF CORK OAK LANDSCAPES	ECO
13-2010	Michael Ahlheim, Oliver Frör, Antonia Heinke, Nguyen Minh Duc, and Pham Van Dinh	LABOUR AS A UTILITY MEASURE IN CONTINGENT VALUATION STUDIES – HOW GOOD IS IT REALLY?	ECO
14-2010	Julian P. Christ	THE GEOGRAPHY AND CO-LOCATION OF EUROPEAN TECHNOLOGY-SPECIFIC CO-INVENTORSHIP NETWORKS	IK
15-2010	Harald Degner	WINDOWS OF TECHNOLOGICAL OPPORTUNITY DO TECHNOLOGICAL BOOMS INFLUENCE THE RELATIONSHIP BETWEEN FIRM SIZE AND INNOVATIVENESS?	IK
16-2010	Tobias A. Jopp	THE WELFARE STATE EVOLVES: GERMAN KNAPPSCHAFTEN, 1854-1923	HCM
17-2010	Stefan Kirn (Ed.)	PROCESS OF CHANGE IN ORGANISATIONS THROUGH eHEALTH	ICT
18-2010	Jörg Schiller	ÖKONOMISCHE ASPEKTE DER ENTLOHNUNG UND REGULIERUNG UNABHÄNGIGER VERSICHERUNGSVERMITTLER	HCM
19-2010	Frauke Lammers, Jörg Schiller	CONTRACT DESIGN AND INSURANCE FRAUD: AN EXPERIMENTAL INVESTIGATION	HCM
20-2010	Martyna Marczak, Thomas Beissinger	REAL WAGES AND THE BUSINESS CYCLE IN GERMANY	ECO
21-2010	Harald Degner, Jochen Streb	FOREIGN PATENTING IN GERMANY, 1877-1932	IK
22-2010	Heiko Stüber, Thomas Beissinger	DOES DOWNWARD NOMINAL WAGE RIGIDITY DAMPEN WAGE INCREASES?	ECO
23-2010	Mark Spoerer, Jochen Streb	GUNS AND BUTTER – BUT NO MARGARINE: THE IMPACT OF NAZI ECONOMIC POLICIES ON GERMAN FOOD CONSUMPTION, 1933-38	ECO

Nr.	Autor	Titel	CC
24-2011	Dhammika Dharmapala, Nadine Riedel	EARNINGS SHOCKS AND TAX-MOTIVATED INCOME-SHIFTING: EVIDENCE FROM EUROPEAN MULTINATIONALS	ECO
25-2011	Michael Schuele, Stefan Kirn	QUALITATIVES, RÄUMLICHES SCHLIEßEN ZUR KOLLISIONSERKENNUNG UND KOLLISIONSVERMEIDUNG AUTONOMER BDI-AGENTEN	ICT
26-2011	Marcus Müller, Guillaume Stern, Ansger Jacob and Stefan Kirn	VERHALTENSMODELLE FÜR SOFTWAREAGENTEN IM PUBLIC GOODS GAME	ICT
27-2011	Monnet Benoit, Patrick Gbakoua and Alfonso Sousa-Poza	ENGEL CURVES, SPATIAL VARIATION IN PRICES AND DEMAND FOR COMMODITIES IN CÔTE D'IVOIRE	ECO
28-2011	Nadine Riedel, Hannah Schildberg-Hörisch	ASYMMETRIC OBLIGATIONS	ECO
29-2011	Nicole Waidlein	CAUSES OF PERSISTENT PRODUCTIVITY DIFFERENCES IN THE WEST GERMAN STATES IN THE PERIOD FROM 1950 TO 1990	IK
30-2011	Dominik Hartmann, Atilio Arata	MEASURING SOCIAL CAPITAL AND INNOVATION IN POOR AGRICULTURAL COMMUNITIES. THE CASE OF CHÁPARRA - PERU	IK
31-2011	Peter Spahn	DIE WÄHRUNGSKRISENUNION DIE EURO-VERSCHULDUNG DER NATIONALSTAATEN ALS SCHWACHSTELLE DER EWU	ECO
32-2011	Fabian Wahl	DIE ENTWICKLUNG DES LEBENSSTANDARDS IM DRITTEN REICH – EINE GLÜCKSÖKONOMISCHE PERSPEKTIVE	ECO
33-2011	Giorgio Triulzi, Ramon Scholz and Andreas Pyka	R&D AND KNOWLEDGE DYNAMICS IN UNIVERSITY-INDUSTRY RELATIONSHIPS IN BIOTECH AND PHARMACEUTICALS: AN AGENT-BASED MODEL	IK
34-2011	Claus D. Müller-Hengstenberg, Stefan Kirn	ANWENDUNG DES ÖFFENTLICHEN VERGABERECHTS AUF MODERNE IT SOFTWAREENTWICKLUNGSVERFAHREN	ICT
35-2011	Andreas Pyka	AVOIDING EVOLUTIONARY INEFFICIENCIES IN INNOVATION NETWORKS	IK
36-2011	David Bell, Steffen Otterbach and Alfonso Sousa-Poza	WORK HOURS CONSTRAINTS AND HEALTH	HCM
37-2011	Lukas Scheffknecht, Felix Geiger	A BEHAVIORAL MACROECONOMIC MODEL WITH ENDOGENOUS BOOM-BUST CYCLES AND LEVERAGE DYNAMICS	ECO
38-2011	Yin Krogmann, Ulrich Schwalbe	INTER-FIRM R&D NETWORKS IN THE GLOBAL PHARMACEUTICAL BIOTECHNOLOGY INDUSTRY DURING 1985–1998: A CONCEPTUAL AND EMPIRICAL ANALYSIS	IK

Nr.	Autor	Titel	CC
39-2011	Michael Ahlheim, Tobias Börger and Oliver Frör	RESPONDENT INCENTIVES IN CONTINGENT VALUATION: THE ROLE OF RECIPROCITY	ECO
40-2011	Tobias Börger	A DIRECT TEST OF SOCIALLY DESIRABLE RESPONDING IN CONTINGENT VALUATION INTERVIEWS	ECO
41-2011	Ralf Rukwid, Julian P. Christ	QUANTITATIVE CLUSTERIDENTIFIKATION AUF EBENE DER DEUTSCHEN STADT- UND LANDKREISE (1999-2008)	IK

Nr.	Autor	Titel	CC
42-2012	Benjamin Schön, Andreas Pyka	A TAXONOMY OF INNOVATION NETWORKS	IK
43-2012	Dirk Foremny, Nadine Riedel	BUSINESS TAXES AND THE ELECTORAL CYCLE	ECO
44-2012	Gisela Di Meglio, Andreas Pyka and Luis Rubalcaba	VARIETIES OF SERVICE ECONOMIES IN EUROPE	IK
45-2012	Ralf Rukwid, Julian P. Christ	INNOVATIONSPOTENTIALE IN BADEN-WÜRTTEMBERG: PRODUKTIONSCLUSTER IM BEREICH „METALL, ELEKTRO, IKT“ UND REGIONALE VERFÜGBARKEIT AKADEMISCHER FACHKRÄFTE IN DEN MINT-FÄCHERN	IK
46-2012	Julian P. Christ, Ralf Rukwid	INNOVATIONSPOTENTIALE IN BADEN-WÜRTTEMBERG: BRANCHENSPEZIFISCHE FORSCHUNGS- UND ENTWICKLUNGSAKTIVITÄT, REGIONALES PATENTAUFKOMMEN UND BESCHÄFTIGUNGSSTRUKTUR	IK
47-2012	Oliver Sauter	ASSESSING UNCERTAINTY IN EUROPE AND THE US - IS THERE A COMMON FACTOR?	ECO
48-2012	Dominik Hartmann	SEN MEETS SCHUMPETER. INTRODUCING STRUCTURAL AND DYNAMIC ELEMENTS INTO THE HUMAN CAPABILITY APPROACH	IK
49-2012	Harold Paredes-Frigolett, Andreas Pyka	DISTAL EMBEDDING AS A TECHNOLOGY INNOVATION NETWORK FORMATION STRATEGY	IK
50-2012	Martyna Marczak, Víctor Gómez	CYCLICALITY OF REAL WAGES IN THE USA AND GERMANY: NEW INSIGHTS FROM WAVELET ANALYSIS	ECO
51-2012	André P. Slowak	DIE DURCHSETZUNG VON SCHNITTSTELLEN IN DER STANDARDSETZUNG: FALLBEISPIEL LADESYSTEM ELEKTROMOBILITÄT	IK
52-2012	Fabian Wahl	WHY IT MATTERS WHAT PEOPLE THINK - BELIEFS, LEGAL ORIGINS AND THE DEEP ROOTS OF TRUST	ECO
53-2012	Dominik Hartmann, Micha Kaiser	STATISTISCHER ÜBERBLICK DER TÜRKISCHEN MIGRATION IN BADEN-WÜRTTEMBERG UND DEUTSCHLAND	IK
54-2012	Dominik Hartmann, Andreas Pyka, Seda Aydin, Lena Klauß, Fabian Stahl, Ali Santircioglu, Silvia Oberegelsbacher, Sheida Rashidi, Gaye Onan and Suna Erginkoç	IDENTIFIZIERUNG UND ANALYSE DEUTSCH-TÜRKISCHER INNOVATIONSNETZWERKE. ERSTE ERGEBNISSE DES TGIN-PROJEKTES	IK
55-2012	Michael Ahlheim, Tobias Börger and Oliver Frör	THE ECOLOGICAL PRICE OF GETTING RICH IN A GREEN DESERT: A CONTINGENT VALUATION STUDY IN RURAL SOUTHWEST CHINA	ECO

Nr.	Autor	Titel	CC
56-2012	Matthias Strifler Thomas Beissinger	FAIRNESS CONSIDERATIONS IN LABOR UNION WAGE SETTING – A THEORETICAL ANALYSIS	ECO
57-2012	Peter Spahn	INTEGRATION DURCH WÄHRUNGSUNION? DER FALL DER EURO-ZONE	ECO
58-2012	Sibylle H. Lehmann	TAKING FIRMS TO THE STOCK MARKET: IPOS AND THE IMPORTANCE OF LARGE BANKS IN IMPERIAL GERMANY 1896-1913	ECO
59-2012	Sibylle H. Lehmann, Philipp Hauber and Alexander Opitz	POLITICAL RIGHTS, TAXATION, AND FIRM VALUATION – EVIDENCE FROM SAXONY AROUND 1900	ECO
60-2012	Martyna Marczak, Víctor Gómez	SPECTRAN, A SET OF MATLAB PROGRAMS FOR SPECTRAL ANALYSIS	ECO
61-2012	Theresa Lohse, Nadine Riedel	THE IMPACT OF TRANSFER PRICING REGULATIONS ON PROFIT SHIFTING WITHIN EUROPEAN MULTINATIONALS	ECO

Nr.	Autor	Titel	CC
62-2013	Heiko Stüber	REAL WAGE CYCLICALITY OF NEWLY HIRED WORKERS	ECO
63-2013	David E. Bloom, Alfonso Sousa-Poza	AGEING AND PRODUCTIVITY	HCM
64-2013	Martyna Marczak, Víctor Gómez	MONTHLY US BUSINESS CYCLE INDICATORS: A NEW MULTIVARIATE APPROACH BASED ON A BAND-PASS FILTER	ECO
65-2013	Dominik Hartmann, Andreas Pyka	INNOVATION, ECONOMIC DIVERSIFICATION AND HUMAN DEVELOPMENT	IK
66-2013	Christof Ernst, Katharina Richter and Nadine Riedel	CORPORATE TAXATION AND THE QUALITY OF RESEARCH AND DEVELOPMENT	ECO
67-2013	Michael Ahlheim, Oliver Frör, Jiang Tong, Luo Jing and Sonna Pelz	NONUSE VALUES OF CLIMATE POLICY - AN EMPIRICAL STUDY IN XINJIANG AND BEIJING	ECO
68-2013	Michael Ahlheim, Friedrich Schneider	CONSIDERING HOUSEHOLD SIZE IN CONTINGENT VALUATION STUDIES	ECO
69-2013	Fabio Bertoni, Tereza Tykvová	WHICH FORM OF VENTURE CAPITAL IS MOST SUPPORTIVE OF INNOVATION? EVIDENCE FROM EUROPEAN BIOTECHNOLOGY COMPANIES	CFRM
70-2013	Tobias Buchmann, Andreas Pyka	THE EVOLUTION OF INNOVATION NETWORKS: THE CASE OF A GERMAN AUTOMOTIVE NETWORK	IK
71-2013	B. Vermeulen, A. Pyka, J. A. La Poutré and A. G. de Kok	CAPABILITY-BASED GOVERNANCE PATTERNS OVER THE PRODUCT LIFE-CYCLE	IK
72-2013	Beatriz Fabiola López Ulloa, Valerie Møller and Alfonso Sousa-Poza	HOW DOES SUBJECTIVE WELL-BEING EVOLVE WITH AGE? A LITERATURE REVIEW	HCM
73-2013	Wencke Gwozdz, Alfonso Sousa-Poza, Lucia A. Reisch, Wolfgang Ahrens, Stefaan De Henauw, Gabriele Eiben, Juan M. Fernández-Alvira, Charalampos Hadjigeorgiou, Eva Kovács, Fabio Lauria, Toomas Veidebaum, Garrath Williams, Karin Bammann	MATERNAL EMPLOYMENT AND CHILDHOOD OBESITY – A EUROPEAN PERSPECTIVE	HCM

Nr.	Autor	Titel	CC
74-2013	Andreas Haas, Annette Hofmann	RISIKEN AUS CLOUD-COMPUTING-SERVICES: FRAGEN DES RISIKOMANAGEMENTS UND ASPEKTE DER VERSICHERBARKEIT	HCM
75-2013	Yin Krogmann, Nadine Riedel and Ulrich Schwalbe	INTER-FIRM R&D NETWORKS IN PHARMACEUTICAL BIOTECHNOLOGY: WHAT DETERMINES FIRM'S CENTRALITY-BASED PARTNERING CAPABILITY?	ECO, IK
76-2013	Peter Spahn	MACROECONOMIC STABILISATION AND BANK LENDING: A SIMPLE WORKHORSE MODEL	ECO
77-2013	Sheida Rashidi, Andreas Pyka	MIGRATION AND INNOVATION – A SURVEY	IK
78-2013	Benjamin Schön, Andreas Pyka	THE SUCCESS FACTORS OF TECHNOLOGY-SOURCING THROUGH MERGERS & ACQUISITIONS – AN INTUITIVE META-ANALYSIS	IK
79-2013	Irene Prostolupow, Andreas Pyka and Barbara Heller-Schuh	TURKISH-GERMAN INNOVATION NETWORKS IN THE EUROPEAN RESEARCH LANDSCAPE	IK
80-2013	Eva Schlenker, Kai D. Schmid	CAPITAL INCOME SHARES AND INCOME INEQUALITY IN THE EUROPEAN UNION	ECO
81-2013	Michael Ahlheim, Tobias Börger and Oliver Frör	THE INFLUENCE OF ETHNICITY AND CULTURE ON THE VALUATION OF ENVIRONMENTAL IMPROVEMENTS – RESULTS FROM A CVM STUDY IN SOUTHWEST CHINA –	ECO
82-2013	Fabian Wahl	DOES MEDIEVAL TRADE STILL MATTER? HISTORICAL TRADE CENTERS, AGGLOMERATION AND CONTEMPORARY ECONOMIC DEVELOPMENT	ECO
83-2013	Peter Spahn	SUBPRIME AND EURO CRISIS: SHOULD WE BLAME THE ECONOMISTS?	ECO
84-2013	Daniel Guffarth, Michael J. Barber	THE EUROPEAN AEROSPACE R&D COLLABORATION NETWORK	IK
85-2013	Athanasios Saitis	KARTELLBEKÄMPFUNG UND INTERNE KARTELLSTRUKTUREN: EIN NETZWERKTHEORETISCHER ANSATZ	IK

Nr.	Autor	Titel	CC
86-2014	Stefan Kirn, Claus D. Müller-Hengstenberg	INTELLIGENTE (SOFTWARE-)AGENTEN: EINE NEUE HERAUSFORDERUNG FÜR DIE GESELLSCHAFT UND UNSER RECHTSSYSTEM?	ICT
87-2014	Peng Nie, Alfonso Sousa-Poza	MATERNAL EMPLOYMENT AND CHILDHOOD OBESITY IN CHINA: EVIDENCE FROM THE CHINA HEALTH AND NUTRITION SURVEY	HCM
88-2014	Steffen Otterbach, Alfonso Sousa-Poza	JOB INSECURITY, EMPLOYABILITY, AND HEALTH: AN ANALYSIS FOR GERMANY ACROSS GENERATIONS	HCM
89-2014	Carsten Burhop, Sibylle H. Lehmann-Hasemeyer	THE GEOGRAPHY OF STOCK EXCHANGES IN IMPERIAL GERMANY	ECO
90-2014	Martyna Marczak, Tommaso Proietti	OUTLIER DETECTION IN STRUCTURAL TIME SERIES MODELS: THE INDICATOR SATURATION APPROACH	ECO
91-2014	Sophie Urmetzer, Andreas Pyka	VARIETIES OF KNOWLEDGE-BASED BIOECONOMIES	IK
92-2014	Bogang Jun, Joongho Lee	THE TRADEOFF BETWEEN FERTILITY AND EDUCATION: EVIDENCE FROM THE KOREAN DEVELOPMENT PATH	IK
93-2014	Bogang Jun, Tai-Yoo Kim	NON-FINANCIAL HURDLES FOR HUMAN CAPITAL ACCUMULATION: LANDOWNERSHIP IN KOREA UNDER JAPANESE RULE	IK
94-2014	Michael Ahlheim, Oliver Frör, Gerhard Langenberger and Sonna Pelz	CHINESE URBANITES AND THE PRESERVATION OF RARE SPECIES IN REMOTE PARTS OF THE COUNTRY – THE EXAMPLE OF EAGLEWOOD	ECO
95-2014	Harold Paredes-Frigolett, Andreas Pyka, Javier Pereira and Luiz Flávio Autran Monteiro Gomes	RANKING THE PERFORMANCE OF NATIONAL INNOVATION SYSTEMS IN THE IBERIAN PENINSULA AND LATIN AMERICA FROM A NEO-SCHUMPETERIAN ECONOMICS PERSPECTIVE	IK
96-2014	Daniel Guffarth, Michael J. Barber	NETWORK EVOLUTION, SUCCESS, AND REGIONAL DEVELOPMENT IN THE EUROPEAN AEROSPACE INDUSTRY	IK

IMPRINT

University of Hohenheim
Dean’s Office of the Faculty of Business, Economics and Social Sciences
Speisemeistereiflügel – 120
70593 Stuttgart | Germany
Fon +49 (0)711 459 22488
Fax +49 (0)711 459 22785
E-mail wiso@uni-hohenheim.de
Web www.wiso.uni-hohenheim.de